ESD-TR-67-615

FIRST QUARTERLY TECHNICAL REPORT – LARGE APERTURE SEISMIC ARRAYS (LASA)

September 1967

DIRECTORATE OF PLANNING AND TECHNOLOGY
ELECTRONIC SYSTEMS DIVISION
AIR FORCE SYSTEMS COMMAND
UNITED STATES AIR FORCE
L. G. Hanscom Field, Bedford, Massachusetts

LEGAL NOTICE

ESD-TR-67-615

FIRST QUARTERLY TECHNICAL REPORT –
LARGE APERTURE SEISMIC ARRAYS (LASA)

September 1967

DIRECTORATE OF PLANNING AND TECHNOLOGY
ELECTRONIC SYSTEMS DIVISION
AIR FORCE SYSTEMS COMMAND
UNITED STATES AIR FORCE
L. G. Hanscom Field, Bedford, Massachusetts

FOREWORD

This research was supported by the Advanced Research Projects Agency. The Electronic Systems Division technical project officer for Contract F19628-67-C-0370 is Major Cleve P. Malone (ESLE).

We wish to acknowledge the very considerable support and assistance that have been provided during the course of this program by the Advanced Research Projects Agency, the Earth Sciences Division of Teledyne, Inc., the Electronic Systems Division Seismic Array Program Office, the Institute for Defense Analyses, the Lincoln Laboratory, and the Vela Seismological Center.

This technical report has been reviewed and is approved.

PAUL W. RIDENOUR, Lt. Col., USAF
Chief, Development Engineering Division
Directorate of Planning and Technology
Electronic Systems Division

ABSTRACT

Four topics are discussed in this Quarterly Progress Report. The first topic relates to the "high-frequency" (4-5 Hz) portion of LASA seismograms. Data are cited which indicate a statistically significant amount of signal energy in this region, and preliminary unsuccessful efforts at combining high-pass filtered records from nearby seismometers are described. The second topic is the problem of detecting underground nuclear tests in the presence of large natural events. A hypothetical detection system consisting of a number of single seismometers at close range and a continental-size array at teleseismic range is analyzed and discussed. The third topic is DIMUS processing of seismic array outputs. The conventional DIMUS processing consists of hardlimiting each seismogram (thereby yielding a one bit per sample representation) and then proceeding as with the unaltered seismograms. Two modified DIMUS schemes, which require a single analog channel, are considered. The performance of these schemes, conventional DIMUS, and conventional analog arrays is evaluated for the spectral-ratio and complexity diagnostics. Finally, an extended version of an automatic pP test is discussed. Initial calculations are presented that suggest that this test will yield satisfactory depth picks for earthquakes as deep as 150 km.

LIST OF FIGURES

TABLE OF CONTENTS

SECTION I

INTRODUCTION

This is the First Quarterly Report on Contract F19628-67-C-0370. The report summarizes the progress on four separate topics: high-frequency seismograms, masking of underground tests with large earthquakes, performance of modified DIMUS processing with discriminant tests, and an extension of the automatic pP test to depths greater than 40 km.

Section II summarizes the results of spectral measurements for twelve events as recorded at three seismometers of LASA. While considerable variation occurs between the various seismometers, most of the events studied were found to possess significant amounts of energy in the 4-5 Hz region. Not enough data are on hand yet to attempt to characterize the spectra of the two classes of events for discriminant possibilities. In addition to the spectral calculations, the high-pass filtered seismograms from several stations were studied to see if it would be possible to improve signal-to-noise ratio by delayed summation of the separate seismograms. Here it was found that the signals are not sufficiently correlated, even over periods as short as one second, to make such addition useful. One of the principal contributors to this lack of correlation was the markedly different predominant periods of the seismic signals on different seismometers separated by no more than 10 km.

Section III discusses two topics related to attempts to hide the signals from an underground test in the signals from nearby, large earthquakes. The first of these topics attempts to describe, as a function of time delay, the region in which a test could be detonated without the resulting signal reaching a network of seismic stations before the signal from the earthquake. The second topic deals with the suppression of the earthquake signal obtainable with an array of continental dimensions. Study of several large events from the Kurile Islands indicates that such an array will reduce energy received from the earthquakes to a level of some 20 dB below that of the direct P arrival within 45 seconds of onset. This reduction is at least 10 dB greater than that obtained with any single one of the seismometers of the array. These facts lead to the hypothesis that if one attempted to conduct a test sufficiently later than the origin time of the earthquake so as to have a large area in which the test might be conducted, the earthquake contribution to the output of the continental array would have decayed sufficiently below its initial level to improve significantly the sensitivity of the array. Thus a combination of the two systems seems called for.

Section IV describes a series of modifications to conventional DIMUS array processing which are intended to reduce distortions of the array output for signals with a high input signal-to-noise ratio. The conventional DIMUS processing consists of hard-limiting each seismogram (thereby yielding a one bit per sample representation) and then proceeding as with the unaltered seismograms. This section also discusses the results of applying two discriminants, complexity and spectral-energy ratio, to the outputs of both analog and modified DIMUS beams for some 24 seismic events.

Briefly, the modifications applied to the DIMUS processing are first the replacement of the DIMUS output with a suitably scaled version of a single analog channel whenever the DIMUS output saturates, and second, the use of the envelope of the analog channel to provide further scaling of the signals processed as described above. This latter modification nearly offsets the severe compression of the signals introduced in the conventional DIMUS.

Based on the two diagnostics examined, it was found that for the seismic events examined, DIMUS-type processors do not significantly degrade classification performance when compared to the analog array. In fact, for each discriminant there was a DIMUS-type processor which did as well as the analog array.

Section V describes the first results obtained with a modified version of the automatic pP depth test. This test was changed from the earlier version so as to include tests for depths as great as 150 km, rather than the previous 40 km limit. As yet, the new test has been applied to only five moderate-depth earthquakes. In addition, only LASA data have been used. For the three events with good signal-to-noise ratios, the test performed quite satisfactorily, despite the limitations imposed by the small size of the LASA array. Further tests are clearly indicated, using arrays with the larger dimensions for which this test was originally designed.

SECTION II

SEISMIC SPECTRA AND HIGH-PASS FILTERED SEISMOGRAMS

The problem of estimating the energy density spectrum of seismic events was analyzed in an earlier report [1] and an estimation procedure was recommended. Using this procedure the energy density spectra for several seismic events were estimated. The results showed a statistically significant amount of signal energy at frequencies as high as 4 or 5 Hz for many of the seismograms. The presence of this "high-frequency" energy has prompted further studies into the possibility that this portion of the spectrum might be useful for seismic discrimination purposes.

There are a few different ways in which the high-frequency portion of the seismic spectra might be useful in discriminating between underground nuclear tests and natural earthquakes. If, for example, the spectra resulting from these two different sources had consistent differences in shape, then some measure of spectral shape might be a useful discriminant. If some measure of the high-frequency energy of the seismic waveform were to be used, the possibility of combining the outputs of several seismometers before performing the spectral calculations should be considered. This question of array processing suggests another general way in which the high-frequency portion of the spectrum might be useful. Since this part of the spectrum corresponds to shorter wavelengths, a given large aperture seismic array would have a narrower beamwidth if it could be successfully operated in the high-frequency region of the spectrum rather than in the region of 1 Hz, which is the dominant frequency of typical short period seismograms. Equivalently, a given beamwidth could be achieved with a smaller aperture if it were possible to exploit the high-frequency region of the spectrum. Whether or not the high-frequency portion of the outputs of several seismometers could be usefully combined depends upon the relations between the wave-forms at the various seismometers. As will be discussed in more detail below, preliminary indications are that there is not sufficient coherence in the high-frequency portion of the spectrum between seismometers separated by a few kilometers to allow any useful array processing.

This section begins with a brief review of previous results. Additional spectral calculations, which are consistent with the earlier results, are also summarized. The question of the coherence across an array of the high-frequency portion of the seismograms is then discussed. Data from two Kazakh events are considered. Examination of the filtered seismograms indicate significant differences in waveshape, dominant frequency, and signal-to-noise ratio. Many of these features may also be observed in the corresponding spectral calculations. These differences are discussed, and it is concluded that they preclude the use of simple delay-sum processing of high-pass filtered seismograms.

2.1 REVIEW AND EXTENSION OF PREVIOUS RESULTS

The method of estimating the energy density spectrum has been discussed in some detail in an earlier report. [2] The basic calculation is fairly easy to describe. The seismogram is multiplied by a time window, which is typically a few seconds long, and the magnitude-squared of the Fourier transform of the resulting waveform is then calculated. If the seismogram is assumed to consist of a desired signal plus additive noise, and this noise is considered to be stationary and Gaussian, the expected contribution of the noise to this spectral calculation may be estimated from a long sample of the noise preceding the onset of the desired signal. The calculated expected noise contribution is called the smoothed periodogram. It is effectively a smoothed version of the power density spectrum of the noise, where the smoothing is chosen to correspond to the smoothing that is implicit in the spectral estimate of the signal. If the seismogram consisted only of noise, the estimate of the energy density spectrum would have an expected value equal to the smoothed periodogram and a variance at each frequency at least as large as the square of the expected value. Thus, a rough criterion for saying that there is a statistically significant amount of signal energy at some frequency would be that the estimate of the energy density spectrum yield a value that is several times larger than the smoothed periodogram at that frequency.

Spectral calculations of this kind were reported earlier for three different seismometer outputs for each of five seismic events.[3] In many of these seismograms, the resulting energy-density-spectrum estimates showed a statistically significant amount of signal energy in the region of 3-5 Hz. These spectral calculations were performed on both unfiltered seismograms and high-pass filtered seismograms, where the high-pass filter attenuated frequencies below 3.75 Hz. The high-pass filter was first employed to exclude the possibility that a "sidelobe" artifact, resulting from the finite duration of the time window, could lead to a spurious high frequency content. Since it is the high frequency portion of the spectrum that is of interest in the current study, the calculations presented below are based on the filtered seismometer outputs. In all cases where the filter is used, it is the same high-pass filter described in the earlier report. The filtering is performed by convolving the filter input with a 1025-point impulse response determined by the following (zero-phase) frequency response.

$$
H(f) = \begin{cases} 0 & |f| < 2.5\text{Hz} \\ 1/2 \ (1-\cos(\frac{2\pi(|f|-2.5)}{2.5})) & 2.5\text{Hz} < |f| < 3.75\text{Hz} \\ 1 & 3.75\text{Hz} < |f| \end{cases}
$$

Similar spectral calculations have recently been performed on twelve additional seismic events, eight of which have epicenters in the Kazakh region. The results of these calculations have been consistent with the calculations reported earlier, and these additional calculations have thus served to confirm the earlier results. Unfortunately, it is still difficult to get earthquakes and surface-focus events of sufficiently comparable magnitudes and epicenters to permit direct comparisons between the shapes of the spectra of these two classes of events. Two of the Kazakh events were larger than 6.0 in magnitude, and the spectral calculations showed evidence of nonlinear distortions in the seismometer-recording system. Three of the Kazakh events had magnitudes between 5.3 and 5.7, and all of these showed a statistically significant amount of high-frequency energy. The remaining three Kazakh events had magnitudes between 4.7 and 4.9, and these events showed little or no high-frequency energy. As with the spectral calculations presented earlier, there was considerable variation between seismometers in the calculated spectra. In the data presented earlier, spectral calculations on a magnitude 5.8 Kazakh event showed a much higher signal-to-noise ratio in the high-frequency region for the center element of the F4 subarray than for those of the A0 and B1 subarrays. A similar tendency was apparent in the spectral calculations on the additional Kazakh events.

2.2   COHERENCE OF THE HIGH-FREQUENCY PORTION OF THE SEISMOGRAM

With a view toward array processing to utilize the high-frequency region of seismic spectra, an attempt was first made to measure the coherence of the high-frequency portion of the seismograms in much the same way as these measurements were made on the unfiltered seismograms in earlier work [4]. There exist techniques for measuring the coherence of the noise as a function of seismometer separation and frequency (see, for example, reference 5), but the method used in these calculations is not directly applicable to measuring the signal coherence since a stationary noise process is assumed, and this allows the combining of calculations performed on several nonoverlapping time intervals.

As a simple first definition of the problem, the array indicated in Figure 2.1 was considered. This array consists of five elements of the existing LASA-Montana, and the separation between pairs of elements varies from 1.5 km to 10.8 km. A large Kazakh surface-focus event was chosen for study. This event is the same one on which spectral calculations were reported earlier. The event was of magnitude 5.8, and the spectral calculations indicated a statistically significant high-frequency content. The outputs of all five seismometers were high-pass filtered using the filter described previously. The question was then asked whether the resulting filtered waveforms could be aligned
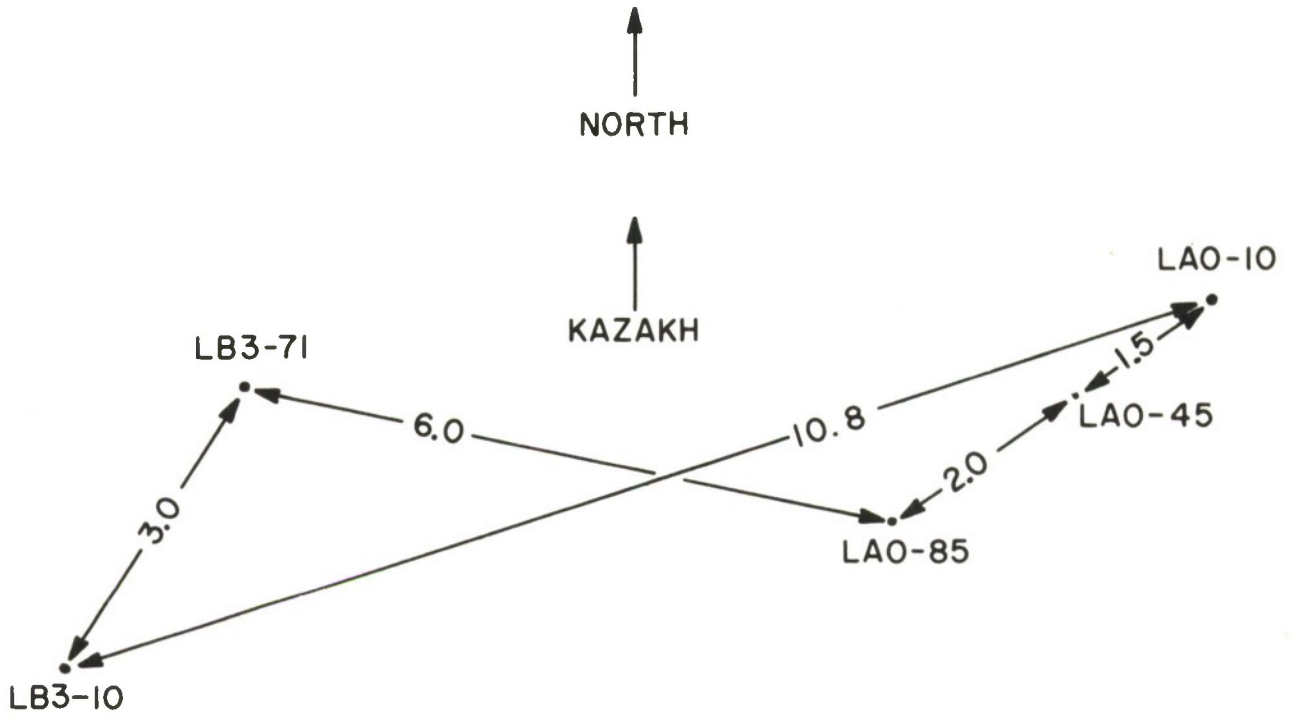
FIGURE 2.1
FIVE ELEMENT ARRAY

in such a way as to lead to a summed seismogram with a signal-to-noise ratio superior to that of any one of the seismograms alone. In considering possible alignments of the seismograms it was, of course, recognized that a different relative timing might be appropriate than was used to align the (predominantly low frequency) unfiltered seismograms. It was hoped that an alignment selected on the basis of this event would also yield satisfactory results for smaller magnitude events from the same region. Since the signals under consideration have most of their spectral energy in the region of 3 to 5 Hz, it was felt that the 20/sec sampling rate was not sufficient to allow proper alignment. For this reason the seismograms were interpolated to yield the equivalent of a 100/sec sampling rate. In other words, relative alignments could be adjusted in 0.01 sec increments rather than the 0.05 sec increments that would be possible with no interpolation. It turned out that it was not possible to align the seismograms in such a way that useful coherence could be achieved, even over an interval of one second in length. The characteristics of the waveforms that preclude this simple array processing will be illustrated below. However, they can be simply summarized by stating that the waveshapes of the high-frequency portion of the seismograms vary widely between seismometers. Even if this were not the case, i.e., if the waveshapes were quite similar, it would be necessary to develop some rule for aligning the seismograms in order to achieve a useful array processing technique. Since the waveshapes differ so significantly, it appears that no alignment scheme will yield useful array processing results, and therefore no operational implementation of the alignment has been considered.

2.3   CHARACTERISTICS OF THE HIGH-PASS FILTERED WAVEFORMS

The original waveforms used in these calculations are presented in Figure 2.2, which is simply a plot of the original 20/sec data. In addition to the five seismograms for the magnitude 5.8 event, another five seismograms from the same five seismometers are presented for a magnitude 5.6 event, also from Kazakh. These ten seismograms are presented on an expanded time scale, after interpolation from 20 to 100 samples per second, in Figure 2.3. Figure 2.4 presents the results of passing the waveforms of Figure 2.3 through the high-pass filter described earlier. The same horizontal scale is used in both Figures 2.3 and 2.4. Several pertinent observations may be made from these figures and some of these can be better understood by examining the appropriate spectral calculations which will be presented in subsequent figures. Also indicated in Figures 2.2-2.4 are the locations of the time windows used in the spectral calculations discussed below.
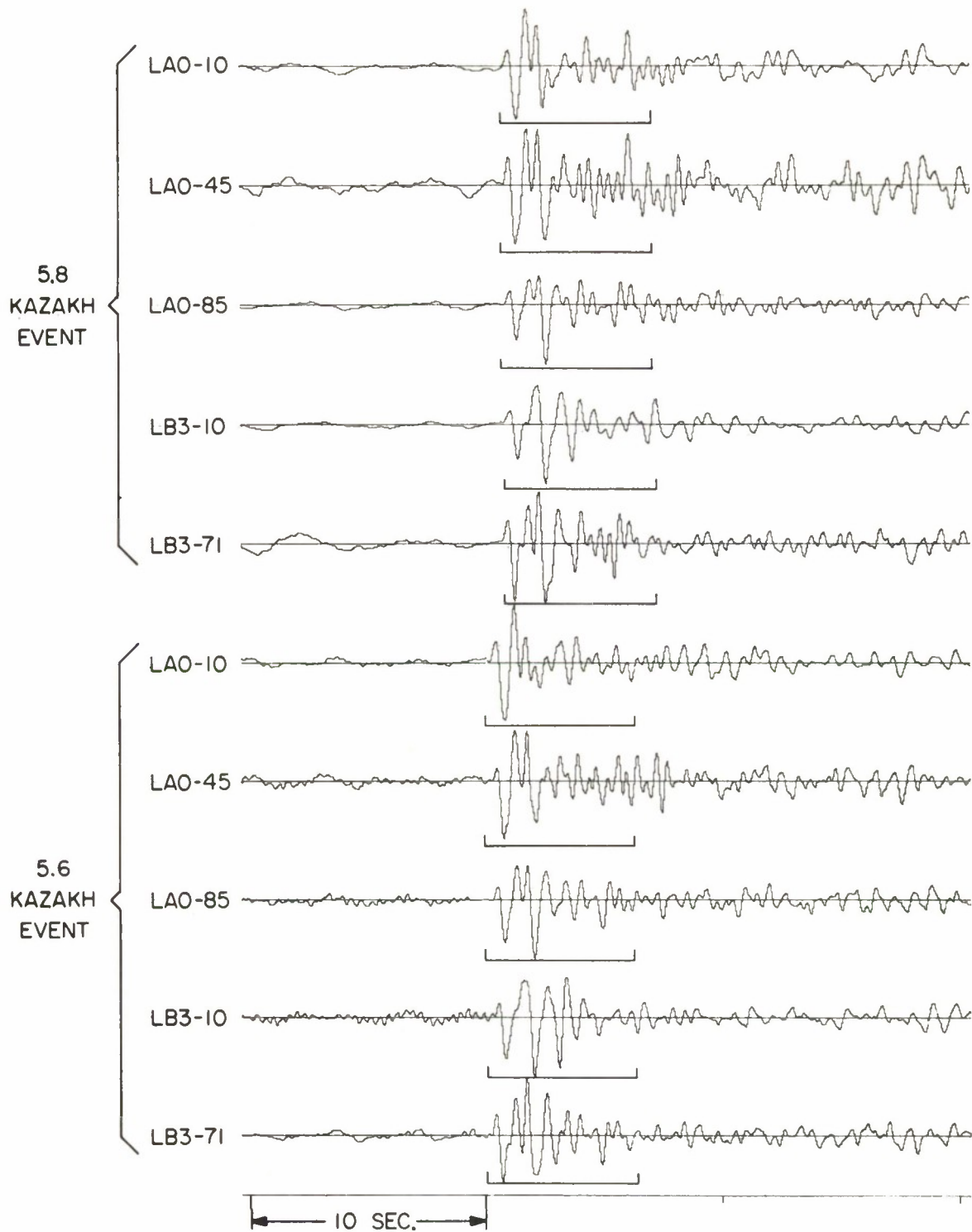
FIGURE 2.2
PLOT OF ORIGINAL (20/SEC) SEISMOGRAMS

It is difficult to find any common features of the five seismograms from the magnitude 5.8 Kazakh event, except those features that would be expected from the limited bandwidth of all five signals. The records were all low-pass filtered at approximately 5 Hz by the aliasing filter before sampling, and the high-pass filtering begins to attenuate at a frequency of 3.75 Hz. Although it is true that all five seismograms have a dominant frequency in the range of 3 to 5 Hz, a close examination indicates that the dominant frequency on each seismogram varies sufficiently among seismograms that coherence over a one-second interval is difficult to achieve. A particularly obvious difference in dominant frequency may be observed by comparing the earlier portion of the A0-10 seismogram with that of the B3-71 seismogram: clearly the A0-10 seismogram has a higher dominant frequency.

Figure 2.5 presents the energy density spectra (solid curves) and smoothed periodograms (dashed curves) for the first five seismograms of Figure 2.4. These calculations were performed using a 128-point Hanning time window with the filtered 20 samples per second data. Before performing these spectral calculations, all of the seismic waveforms were normalized so that the rms value of the unfiltered noise preceding the event was unity. Comparing the spectra for seismogram A0-10 with that for B3-71, it may be noted that the smoothed periodograms are quite similar, but the energy density spectra are very different, reflecting the difference in dominant frequency that is apparent in Figure 2.4. It may also be observed from Figure 2.5 that seismograms A0-10 and B3-10 show relatively more high-frequency content than the other seismograms. These two seismometers are the center elements of their respective clusters and are buried deeper than the other elements. [6] The greater depth of these two might be expected to lower the relative amount of high-frequency noise, but whether or not it is the reason for the relative increase in high-frequency signal energy is not clear. Finally, Figure 2.5 shows that both the signal and noise spectra for A0-45 and A0-85 are quite similar.

Figure 2.6 presents the standard spectral calculations for the magnitude 5.6 event. From Figures 2.3 and 2.6 some similarities and some differences between these two events may be observed. As with the magnitude 5.8 event, the magnitude 5.6 event shows a higher dominant frequency in the A0-10 seismogram than it does in the B3-71 seismogram. In the case of the magnitude 5.8 event, the A0-45 and A0-85 seismograms had quite similar spectra. This is not the case with the magnitude 5.6 event, as is clear in the seismograms of Figure 2.3, where A0-85 shows a poor signal-to-noise ratio. The difference in signal-to-noise ratios is clear in the spectral calculations of Figure 2.6 as well.
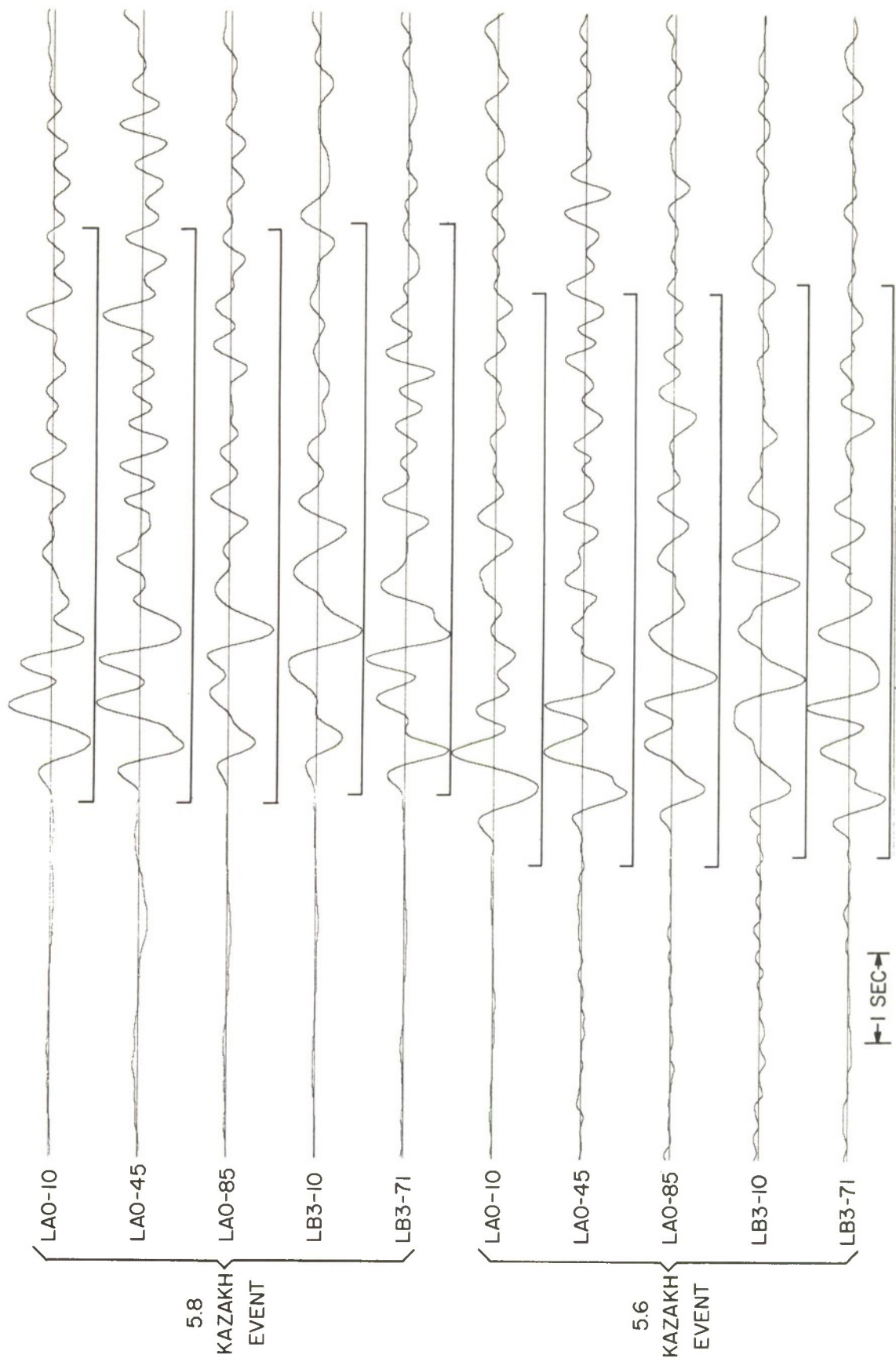
FIGURE 2.3
UNFILTERED, INTERPOLATED SEISMOGRAMS
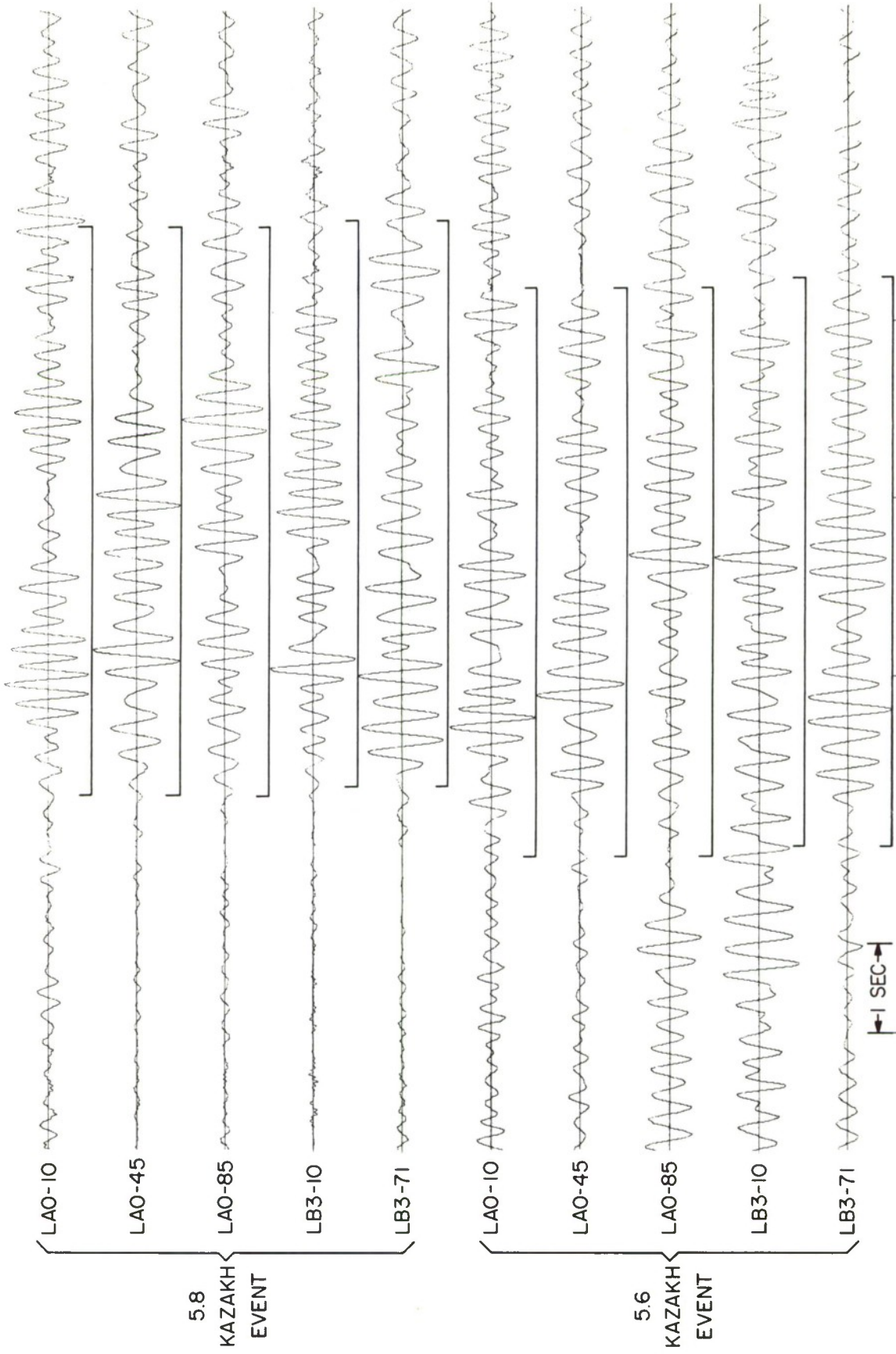
FIGURE 2.4
HIGH-PASS FILTERED, INTERPOLATED SEISMOGRAMS

LAO-IO
LAO-45
LAO-85
LB3-IO
LB3-7I

5.8
KAZAKH
EVENT

LAO-IO
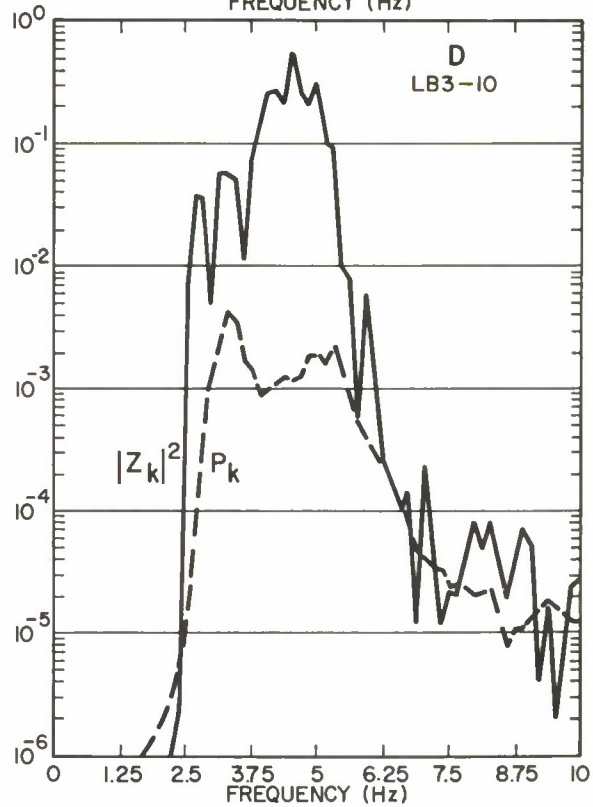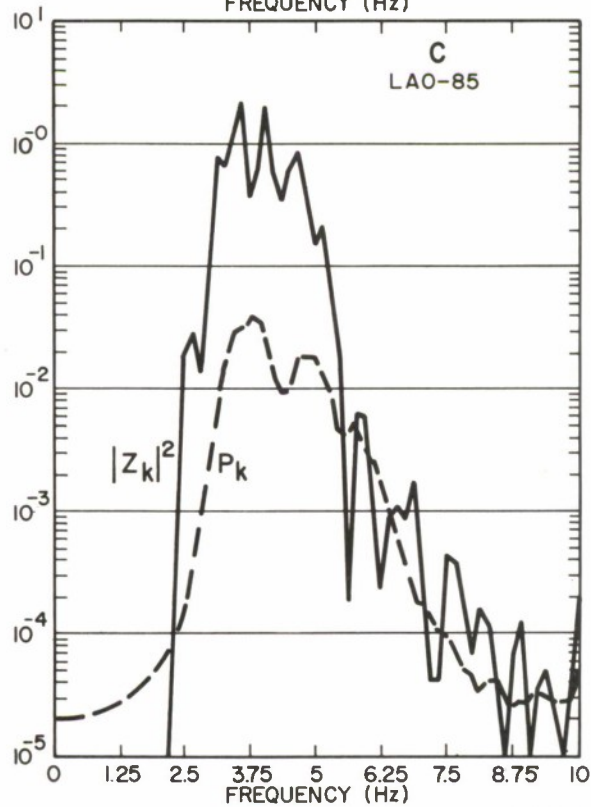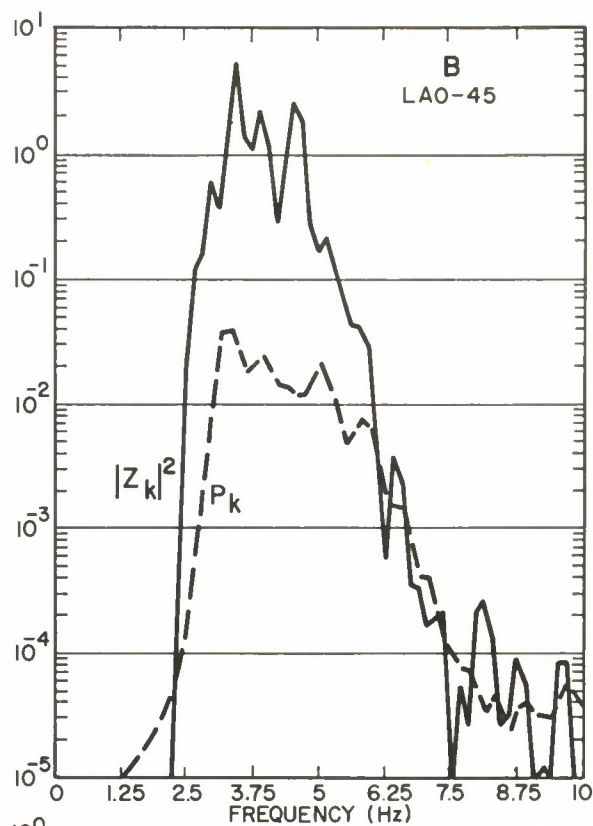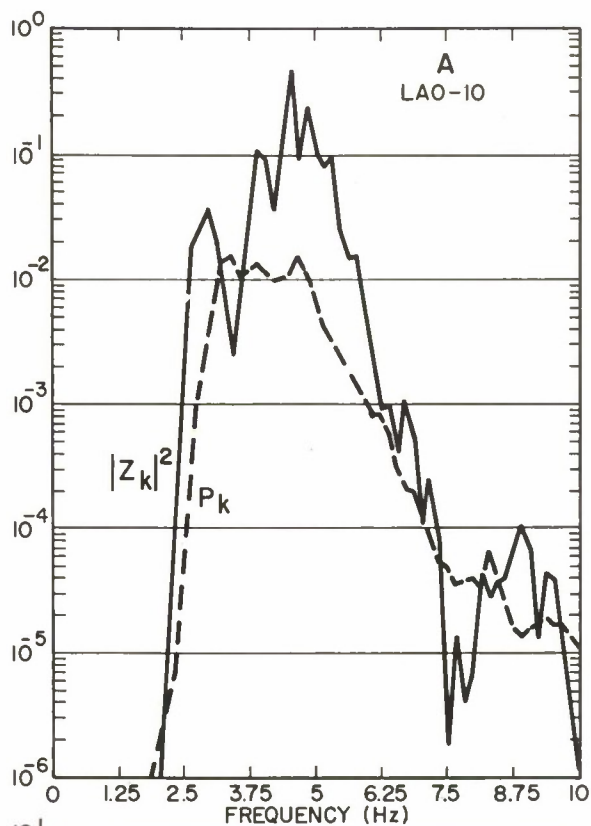LAO-45
LAO-85
LB3-IO
LB3-7I

5.6
KAZAKH
EVENT

I SEC

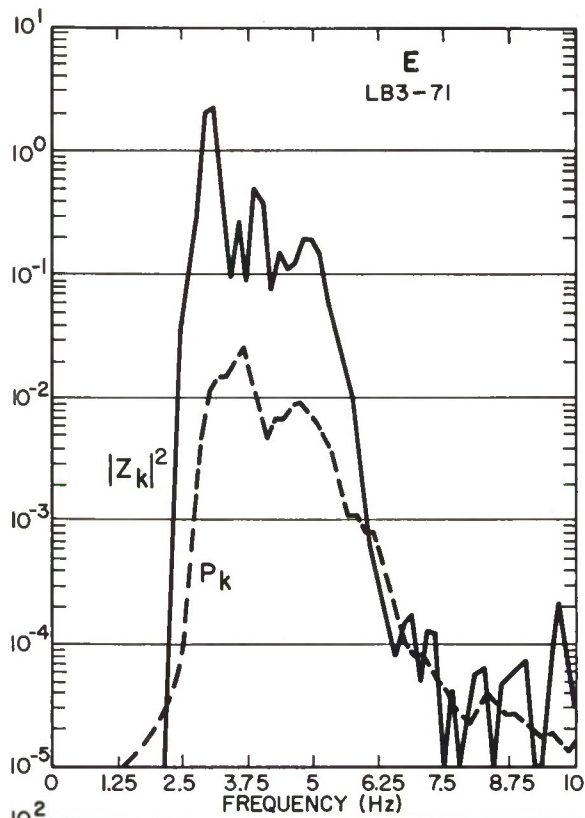FIGURE 2.5 (A-D)
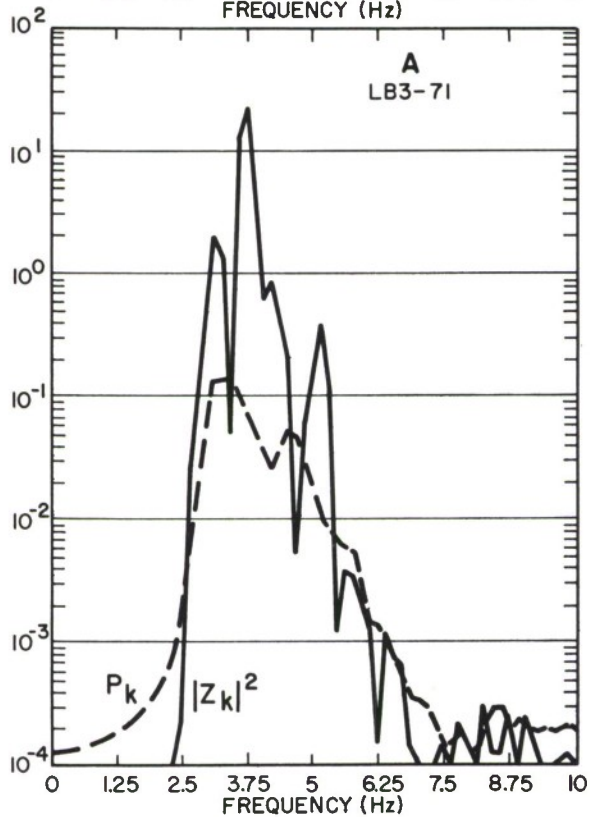SPECTRAL CALCULATIONS 5.8 KAZAKH EVENT

FIGURE 2.5 (E)
SPECTRAL CALCULATIONS 5.8
KAZAKH EVENT

FIGURE 2.6 (A)
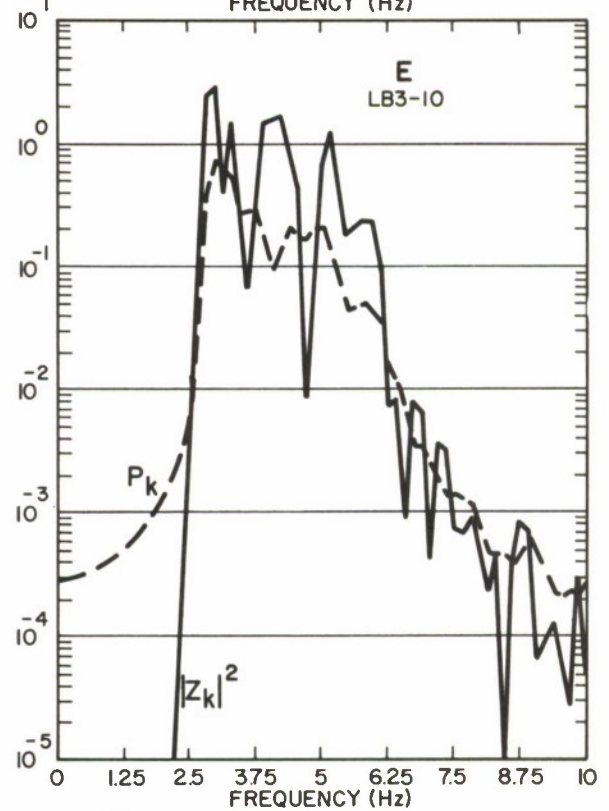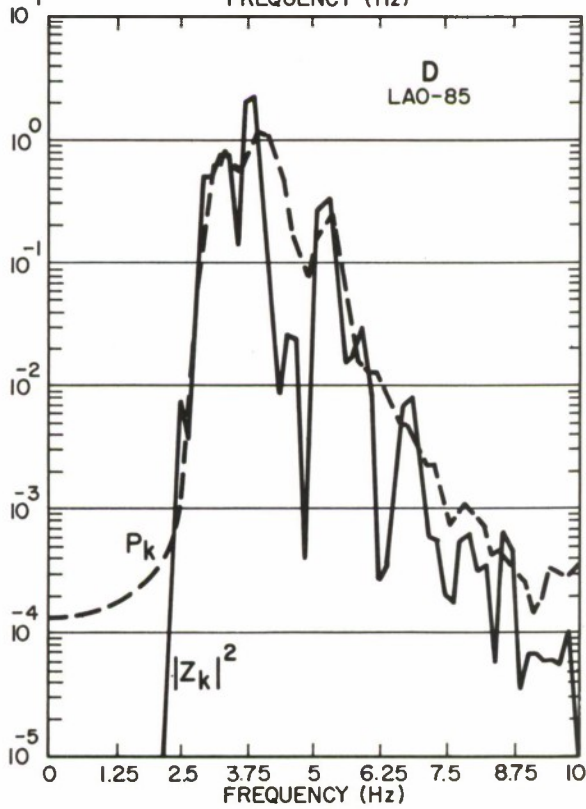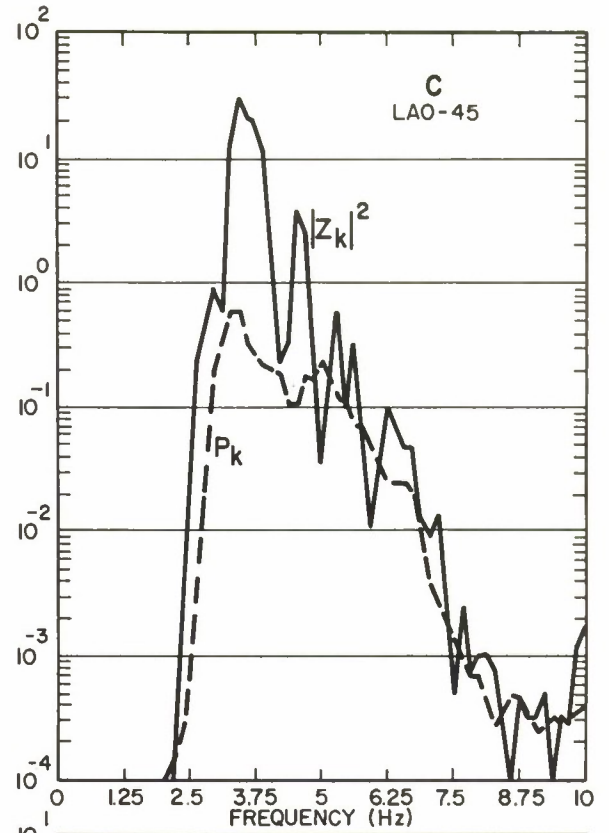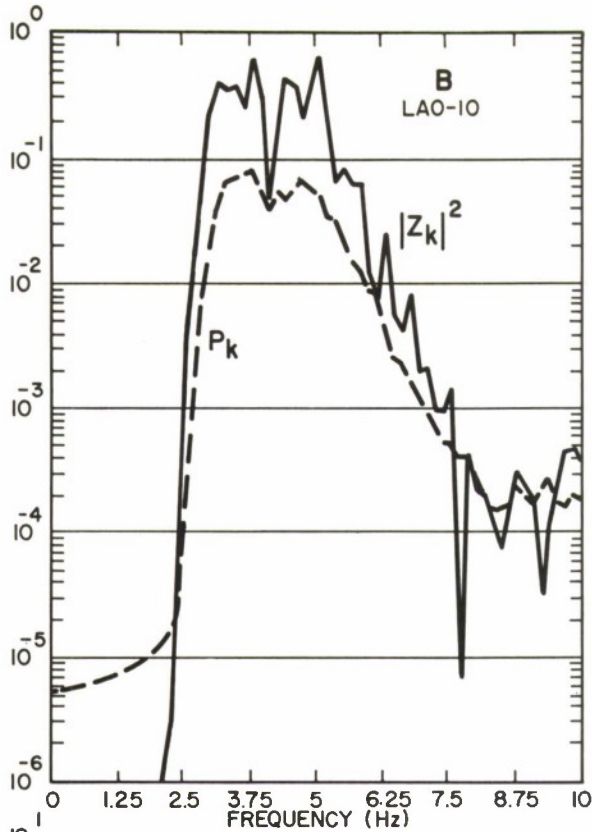SPECTRAL CALCULATIONS 5.6
KAZAKH EVENT

FIGURE 2.6 (B-E)
SPECTRAL CALCULATIONS 5.6 KAZAKH EVENT

In summary, it may be stated that the high-pass filtered seismograms in the cases considered show considerable differences in waveshapes, dominant frequencies, and signal-to-noise ratios even when the unfiltered seismograms look quite similar. Since this is the case, and these differences are sufficient to preclude significant coherence between seismograms over periods as long as one second, it does not appear that delay-sum processing of the high-pass filtered waveforms would lead to useful results either in terms of signal-to-noise enhancement or directional characteristics of the array. It should be stressed that these negative remarks have been made without considering the possible additional problems of adequate signal-to-noise ratio. Even if it had turned out that the waveshapes were quite similar, it would have been necessary to examine the relative sensitivity of a high-frequency array compared to that of the existing array.

There are, of course, many possible explanations for the differences in the high-pass filtered waveforms for seismometers that are separated by a few kilometers. For one thing the detailed amplitude and phase characteristics of the seismometers in the frequency range of interest may vary. Also the local geology may be such as to introduce frequency-dependent amplitude and phase characteristics that vary significantly between seismometer sites. If all of the frequency-dependent differences peculiar to each seismometer site were consistent, and not too sensitive to epicenter, it might be possible to correct the waveforms of each seismometer by some equalization process and then to form an array using the equalized waveforms. This possibility has not been explored except to the extent of trying (unsuccessfully) to find consistencies between the two sets of waveforms given in Figure 2.4.

2.4 SUMMARY AND CONCLUSIONS

A progress report on work directed at using the "high-frequency" portion of seismograms for purposes of seismic discrimination has been presented. Earlier work, reported elsewhere, had suggested a method of estimating the energy density spectra of seismic signals, and calculations based on this method have indicated a statisically significant amount of high-frequency energy in the seismograms resulting from several seismic events. Additional calculations on twelve more seismic events were briefly cited in this report and it was noted that the results were consistent with those reported earlier. Specifically, a significant amount of high-frequency energy was apparent in several of the spectral calculations, and a considerable difference among seismometers has been observed in the detailed spectra resulting from each event. Unfortunately, the existing collection of data has not been sufficient to make apparent any characteristic differences in spectral shapes resulting from the two classes of seismic events.

The possibility of combining the high-frequency portion of several seismograms has been explored during this period. The objective in exploring this possibility is that array processing designed to utilize the high-frequency region might lead to useful discriminants and also to better directional characteristics for a given aperture than is available from arrays using the low-frequency portion of the spectrum. To date only data from two large-magnitude Kazakh events have been considered, using an array consisting of five elements of the existing LASA-Montana that have separations between 1.5 and 10.8 kilometers. Examination of the high-pass filtered outputs of these five seismometers indicates considerable differences in waveshapes, dominant frequencies and signal-to-noise ratios. The difference in spectral content between the high-pass filtered seismograms that is suggested by the seismograms themselves may also be observed in the calculated energy density spectra and smoothed periodograms. The differences between the high-pass filtered outputs are sufficient to suggest that useful coherence between seismometers over a time interval as long as one second cannot be achieved by simple alignment of the high-pass filtered records. Whether or not some more sophisticated processing might be successful in exploiting this portion of the spectrum has yet to be determined.

SECTION III

DETECTION OF NUCLEAR EXPLOSIONS IN THE PRESENCE
OF LARGE NATURAL EVENTS

The problem of detecting an underground nuclear explosion in the proximity of a large earthquake involves many considerations. One approach to this problem -- that of using a continental-size array to search the vicinity of the earthquake epicenter for a possible nuclear test -- was considered in a recent report [7]. The motive for considering a continental size array rather than one of the dimensions of the existing LASA-Montana was simply that the narrower beamwidth of the continental-size array (approximately 1° rather than 10°) would be useful for searching the vicinity of the earthquake epicenter for a possible underground nuclear test. While the continental-size array may be useful, perhaps even essential, in detecting nuclear explosions in the proximity of earthquakes, it represents only one approach to the problem, and in many cases may not be necessary. More specifically, there are many situations in which single seismometers, appropriately distributed about the potential epicenter, would be sufficient to exclude large regions as possible sites of an underground nuclear test. In an operational system this would be most valuable since it would reduce the area that would have to be "searched" by the continental-size array.

We shall first consider a system consisting of a set of single seismometer stations located at a relatively short range from the earthquake's epicenter and well distributed in azimuth. If the single seismometer stations surround the earthquake epicenter, it is possible to place limits on how soon after the earthquake origin time an underground nuclear test could be detonated without being detected by one of these single seismometer stations. In this analysis it is assumed that if the signal from the underground nuclear test were to arrive at any one of the several seismometers before the earthquake signal, appropriate processing of the seismometer data would indicate that a nuclear test had taken place. Using standard travel-time tables it is straightforward to calculate, as a function of position relative to the earthquake epicenter, the minimum time delay between the earthquake and the nuclear test that is necessary to avoid the detection in the manner just described. The results of these calculations will be presented as contour plots indicating areas of possible concealment for different values of minimum delay. The motive for presenting these calculations in this way was suggested earlier: it is only the area of possible concealment which surrounds the earthquake epicenter that must be searched by a large aperture seismic array, since at a given time after the earthquake all of the areas outside of the corresponding area of possible concealment can be excluded as possible test sites on the basis of the single seismometer outputs.

The second major topic to be considered is the characteristics of continental-size arrays as measured with actual seismic data. As noted above, the continental-size array would be used for searching the areas of possible concealment. We shall briefly comment on the relative merits of a continental-size array and a LASA in this context. The complete detection system considered here consists of a single large aperture seismic array (probably of continental dimensions) plus a collection of single stations. In order to give some indication of the possible performance of both single seismometers and continental-size arrays of seismometers in detecting underground nuclear tests in the presence of earthquake signals, several calculations are presented of the average energy per unit time as a function of time after the earthquake arrival for both single seismometers and continental-size arrays consisting of these seismometers. Although they are highly variable, the results of these calculations give some indication of what might be the minimum detectable nuclear test as a function of the delay between the earthquake onset and the detonation of the test. In general, of course, the more time that has elapsed since the earthquake, the better job that the seismic array can do of detecting a nuclear test. From the point of view of trying to hide a nuclear test in the earthquake signal, these calculations suggest a maximum allowable delay between the earthquake and the detonation of the test that depends upon the magnitudes of both. In contrast, the earlier considerations -- those involving the signal seismometers surrounding the earthquake epicenter -- impose a minimum time delay between the earthquake and the nuclear test detonation.

3.1   REGIONS OF POSSIBLE CONCEALMENT

A set of single seismometer stations surrounding an earthquake epicenter significantly limits the region in which an underground nuclear test could be set off without risking detection by one of these seismometers. In this section, one sample calculation is presented in order to indicate the degree of this limitation. As indicated above, the assumption on which this calculation is based is the following: if the first arrival from the underground nuclear test precedes that of the earthquake at any one of the seismometers, then the test is considered not to have been concealed. The rationale behind this criterion is that if two arrivals at a given seismometer appear, and there is no evidence to suggest two earthquakes, further studies of the available seismograms would be indicated. And, even if the first arrival from the nuclear test were mistaken for that of an earthquake, attempts to find an earthquake epicenter that is consistent with all of the arrival times would fail, and this, in turn, would suggest that further study was in order.

It is instructive to consider a few examples of the dependence of this sort of detection system on the range from the individual seismometers to the two epicenters of interest. For a given pair of epicenters, the seimometers that determine the minimum delay between the earthquake and the nuclear test

are those that are closer to the test site than to the earthquake epicenter. The minimum delay imposed by any single seismometer is, of course, the difference in travel times to the seismometer from the earthquake epicenter and the test site. For the case where the two epicenters are relatively close together, the derivatives of standard travel-time tables provide the appropriate measure of sensitivity. For a seismometer at a range of 10° the derivative has a value of 13.7 sec/degree. For a seismometer at 104° the derivative is only 4.4 sec/degree. The shape of the travel-time curves strongly favors having seismometers at relatively close ranges to the epicenter. For example, a set of seismometers surrounding the earthquake epicenter at a range of approximately 20° (at which the derivative of the travel-time table is approximately 10 sec/degree) would limit the region of possible concealment to a circle with a radius of approximately 1° for a minimum delay time of 10 sec. A delay time of 30 sec would limit the area of possible concealment to a circle of 3° in radius.

For the regions of interest, the present world-wide seismograph stations (WWSSS) are in general not at a range of 20° or less and therefore do not reduce the area of possible concealment to the dimensions of 1° or 3° just cited. An example of the areas that do occur with the existing WWSSS has been calculated assuming an earthquake epicenter in Mongolia, where several large earthquakes have occurred in the past. It should be noted that this calculation, which will be described in more detail below, does not involve any actual seismic waveforms. The calculation is based entirely on the location of the earthquake epicenter and the seismometers. A set of 18 stations of the WWSSS was assumed for these calculations. These stations are well distributed in azimuth and are among the closest to the epicenter.

The calculation of areas of possible concealment for different delays may be described as follows: a map is constructed with the earthquake epicenter at its center and several grid points surrounding this epicenter. In the data to be presented below, these grid points are separated by one degree increments in range and 30 degree increments in azimuth. Each grid point is considered as a possible test site. For each grid point the travel time to each of the seismometers is calculated and subtracted from the corresponding travel time from the earthquake epicenter to each seismometer. The largest positive number resulting from this calculation specifies the minimum delay time corresponding to that grid point. In other words, if a nuclear test were set off at that grid point less than the indicated number of seconds after the earthquake, there would be at least one seismometer at which the signal from the nuclear test would be received before the signal from the earth-

quake. Once this calculation has been performed for all of the grid points, contours are drawn indicating approximately the regions corresponding to certain minimum delay times. For example, using the stations indicated in Figure 3.1 and assuming an earthquake epicenter in Mongolia, the contour map of Figure 3.2 has been calculated. It may be observed from this figure that the area of possible concealment for a delay of 30 sec, varies between 2.5° and 4.5° in range from the epicenter. The 60 sec contour from Figure 3.2 also appears on the map of Figure 3.1, for the epicenter under consideration.

3.2   ENERGY DECAY RATES

The immediately preceding discussion indicates limits on the region about an earthquake epicenter in which an underground nuclear test could be detonated without risk of detection by a single seismometer. These limits are a function of the delay time between the earthquake and the nuclear test, with the region of possible concealment growing in size with increasing delay time. These calculations in no way depend on the magnitude of either the earthquake or the shot, because the simple assumption is made that the shot would be detected if its signal arrived at any seismometer before the earthquake signal arrived at that seismometer. Having reduced the problem to the areas of possible concealment, the questions still remain as to what technique to use to search for a nuclear test in these regions and how sensitive such a technique would be.

In an earlier report, beam patterns for continental-size arrays were presented. [8] These patterns were based on actual locations of seismometers, but the calculations assumed that the seismic signal consisted of one period of a 1 Hz sinewave. Such an assumption is relevant when considering the ability of the array to accept or reject the (highly correlated) P-phase of a seismic signal. However, the calculated array pattern has little relevance in considering the array output during the coda of the earthquake signal. The reason for this is that for seismometer separations of several hundred kilometers, the coda is relatively uncorrelated between seismometers and in terms of considering the characteristics of the seismic array, then, the coda could be regarded simply as independent noise at each receiving element. In this situation, the clearest reason for using a very large aperture seismic array is that it does reduce the correlation of the coda between the various seismometers.

Using actual data from two large earthquakes, the average power has been calculated as a function of the time after the earthquake for both single seismometers and continental-size arrays. The array output is formed by normalizing all of the seismograms to the same P-phase energy, aligning the seismograms
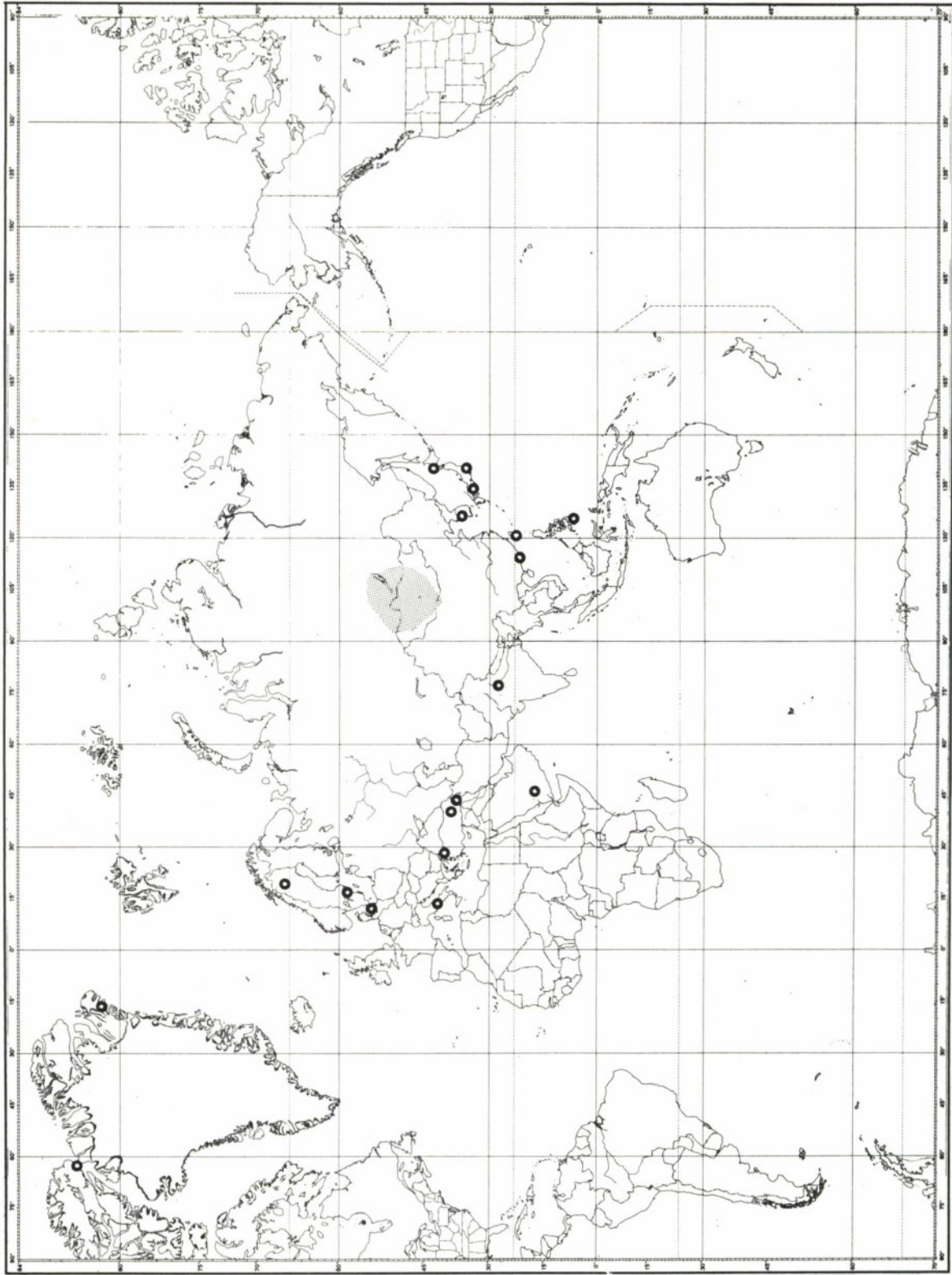
FIGURE 3.1

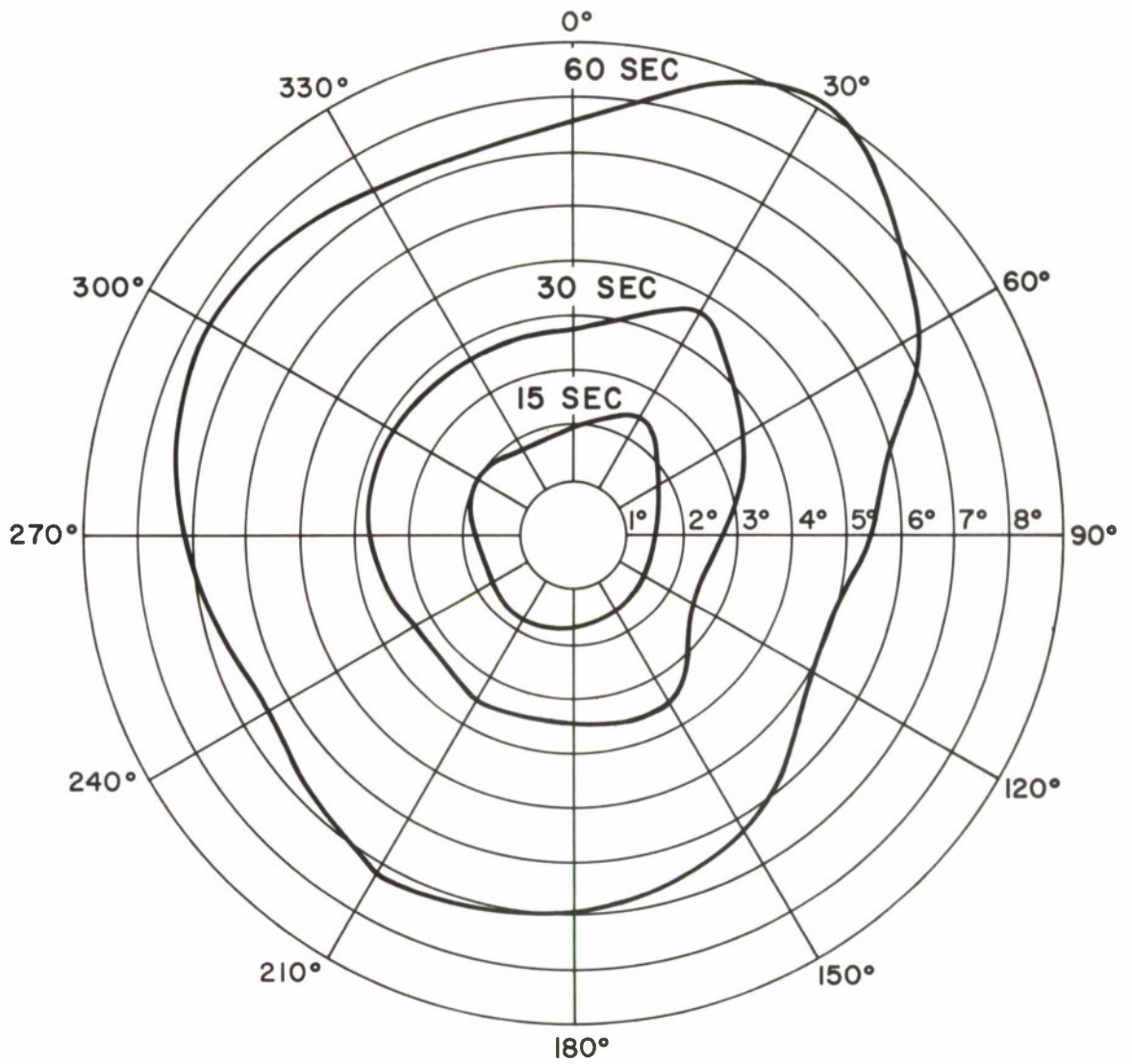MAP SHOWING LOCATION OF STATIONS AND THE 60 SEC. CONTOUR

FIGURE 3.2

EXAMPLE OF AREAS OF POSSIBLE
CONCEALMENT FOR DIFFERENT DELAYS

on the P-phase arrival, and summing. In these calculations, the
energy is calculated for each of 150 consecutive 1 sec intervals,
and the result is plotted on a semi-logarithmic scale. The rea-
son for performing this calculation is that it gives some indi-
cation of how large the signal from an underground nuclear test
would have to be in order to be detected in the presence of this
earthquake signal. It turns out in the data to be presented that
the decay rate of the energy per unit time is appreciably higher
for the continental-size array than it is for a single seismometer.
This fact alone says that the continental-size array is useful
in that a given magnitude nuclear test is more likely to show
up as a large excursion in the energy per unit time out of the
array than it is at a single seismometer. Presumably, if the
array were to be used to search the region of possible conceal-
ment for a nuclear test, it would be focused at each of the
several cells with dimensions corresponding to the beamwidth of
the array pattern. Given that the array is focused at a possible
test site, the waveform from the test, if it exists, should con-
tribute a coherent component at all of these seismometers. If
the time since the earthquake were small enough that the earth-
quake waveform is still coherent at the various seismometers,
the array pattern for the continental-size array would be relevant.
If, however, sufficient time has elapsed that the earthquake
contribution at the various seismometers is incoherent, then
the energy out of the array may be estimated from the energy
plots given below. It should be noted that if the contribution
of each seismometer is incoherent, the same average energy as
a function of time would be expected whether the array is aimed
at the earthquake epicenter or elsewhere.

3.2.1   Experimental Results

Data from two earthquakes with epicenters in the Aleu-
tian Islands region have been processed in the manner just
described, and the results appear in Figures 3.3-3.6. Infor-
mation concerning these data is summarized in the following
table.

Date	Mag.	Depth	No. of Stations
17 March 1965	6.0	23 km	12
1 September 1964	5.5	25 km	15

Both earthquakes were impulsive, rather than emergent. This
selection was deliberate and was motivated by the thought that
it would be easier to characterize the impulsive data. Even-
tually, the emergent data will also have to be considered. The
station selection was rather arbitrary and was primarily deter-
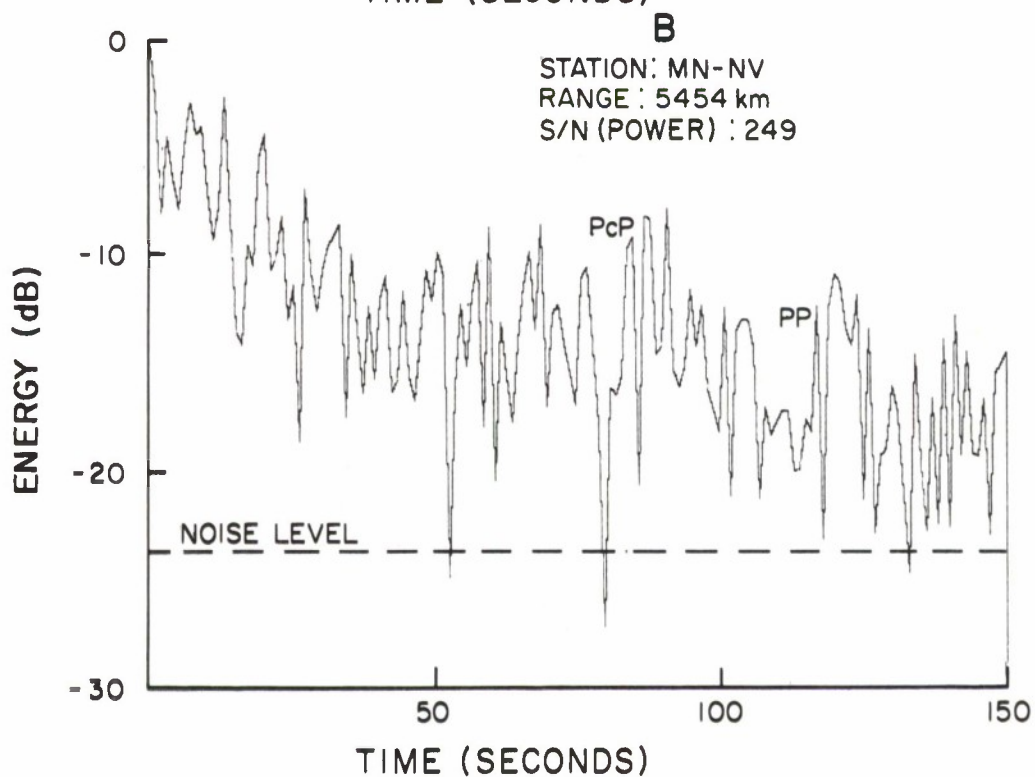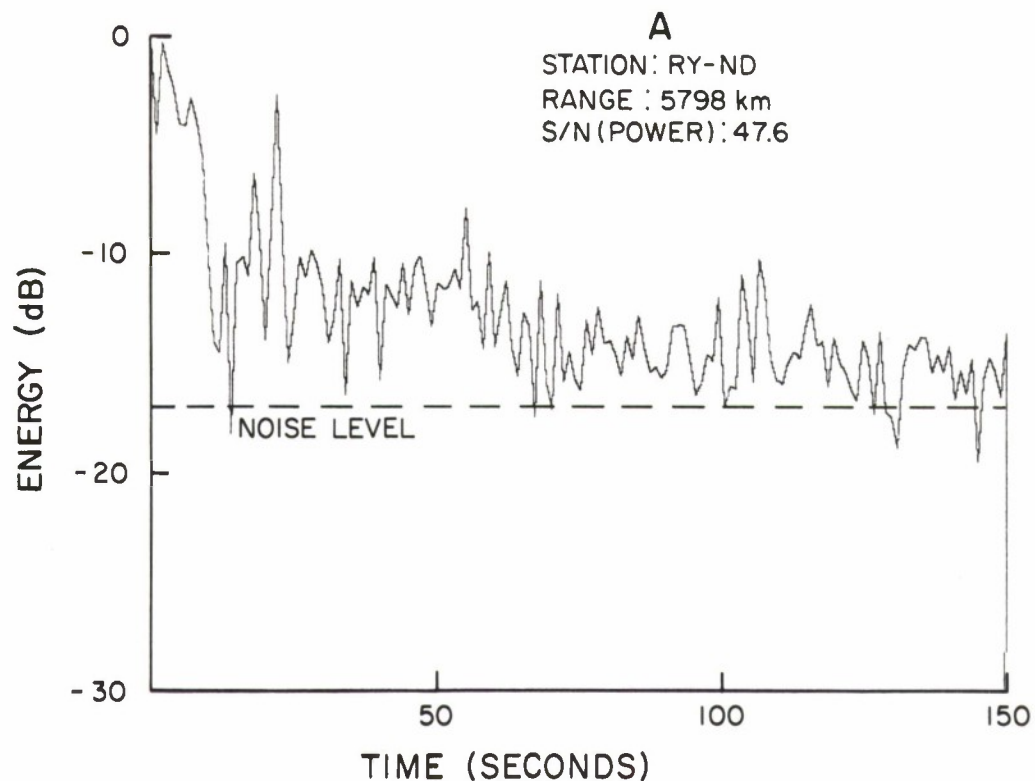mined by the availability of "good" seismograms for these two
events.

FIGURE 3.3 (A-B)
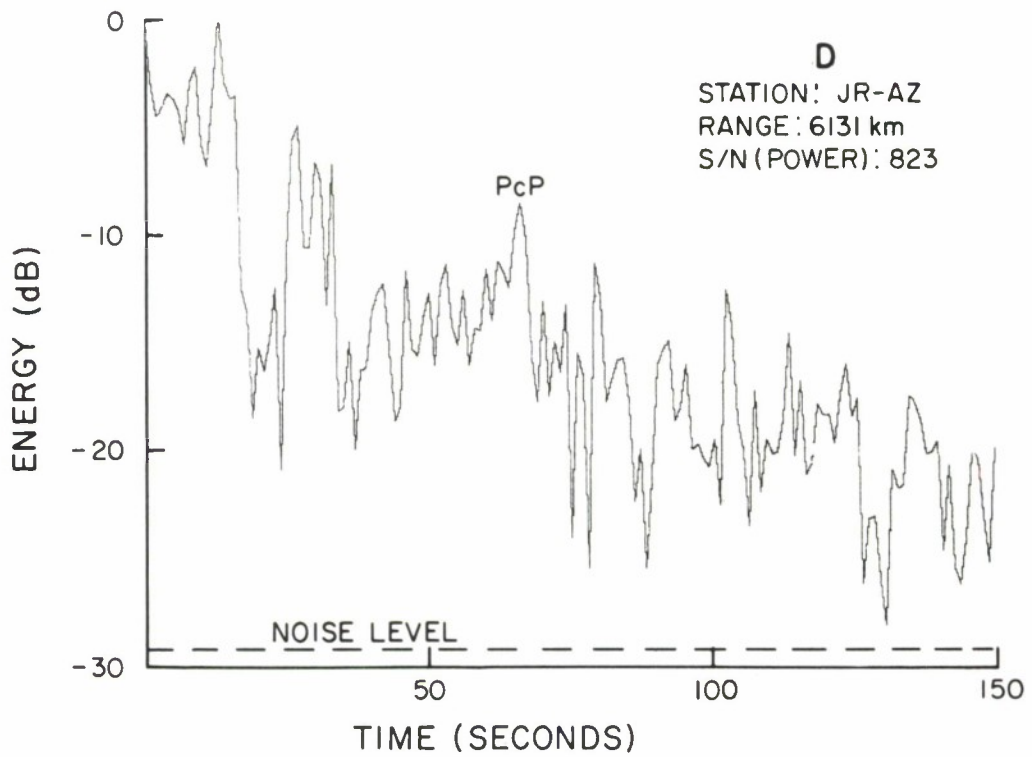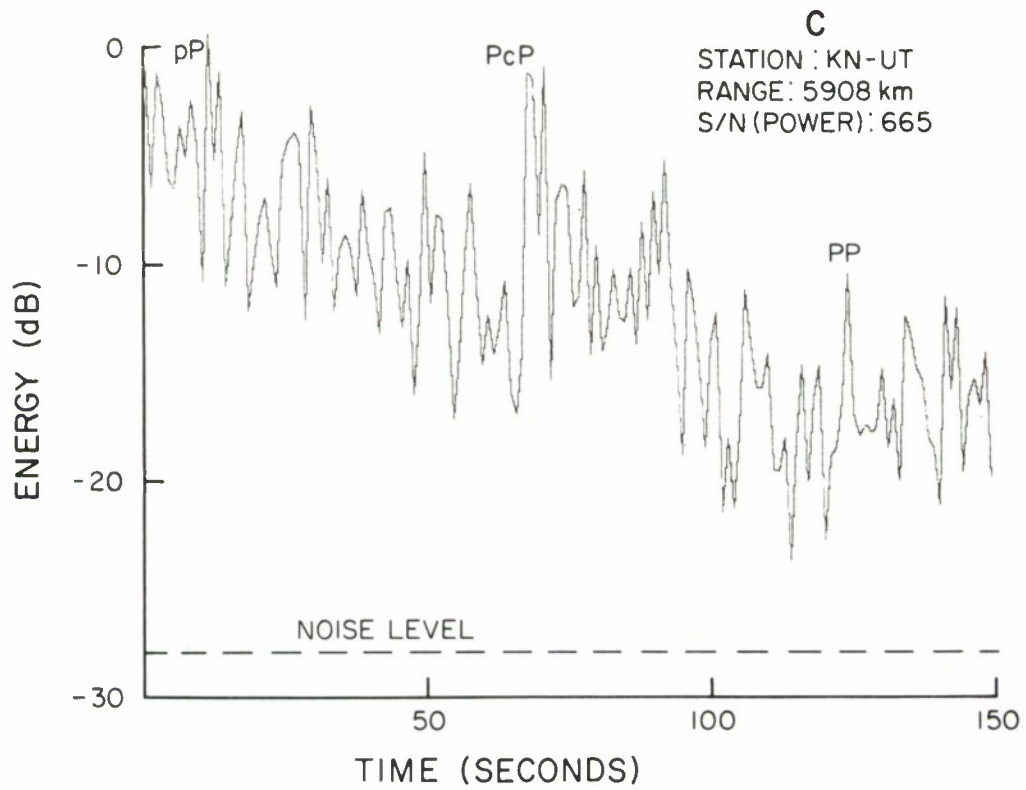ENERGY VS. TIME FOR SELECTED STATIONS (17 MAR 65 EVENT)

FIGURE 3.3 (C-D)
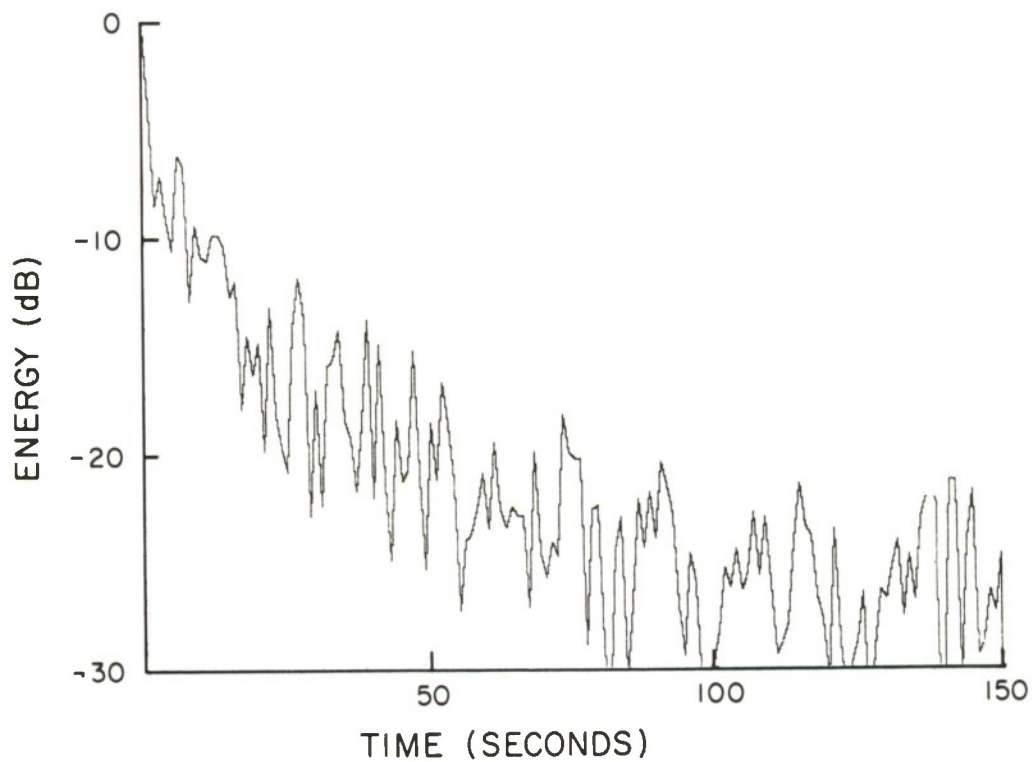ENERGY VS. TIME FOR SELECTED STATIONS (17 MAR. 65 EVENT)

FIGURE 3.4

ENERGY VS. TIME FOR PHASED SUM (17 MAR 65 EVENT)

For the 17 March 1965 event the signal-to-noise (power) ratio (defined as the ratio of the energy in the first one second of the "signal" to the average power in the noise preceding the signal) varies between stations from 21.1 for VOIO to 823 for JRAZ. Only eight stations had a signal-to-noise ratio larger than 100.

The twelve stations used with the event varied in range from 50° to 65°. With these ranges, the phases that would be expected in the 150 sec interval used for the calculations are P, pP, sP, PcP, and PP. In some cases, these phases are apparent in the energy-time plots and are labeled accordingly.

Figure 3.3 shows the energy as a function of time for four representative stations. From this figure it may be observed that for the stations with a low signal-to-noise ratio, the energy curve decays to approximately the noise level within the 150 sec plotted, but this is not at all the case for the high signal-to-noise ratio stations.

From Figure 3.3 it would appear that a seismic event that was one magnitude unit (20 dB) smaller than the earthquake, and arrived within 150 sec following it, would not lead to an identifiable contribution in any of the single seismometer outputs. In contrast, Figure 3.4 shows the energy decay curve for the output of the continental-size array. This curve shows a more rapid decay than that of the single seismometer. In particular, after approximately 75 sec, the energy of the array output remains at least 20 dB below its initial value.

The 1 September 1964 event was of magnitude 5.5, which is 0.5 magnitude units less than the 17 March event. For this event, a total of 15 seismograms were processed, and nine of these have a signal-to-noise (power) ratio of 100 or more. The ranges of the fifteen stations to the epicenter varied between 38° and 62°.

Figure 3.5 shows the energy decay curves for four representative stations with signal-to-noise ratios ranging from 42.5 to 902. As before, peaks in the energy curves that occur at the correct time for a specific phase (pP, PP, PcP) are appropriately labeled.

Figure 3.6 presents the energy decay curve for the output of the continental-size array found by using all 15 records. As expected, this curve decays more rapidly than those of the individual seismometers. One peculiarity of the curve is the small increase in energy that is apparent in the last 50 seconds. This trend is the result of the PcP
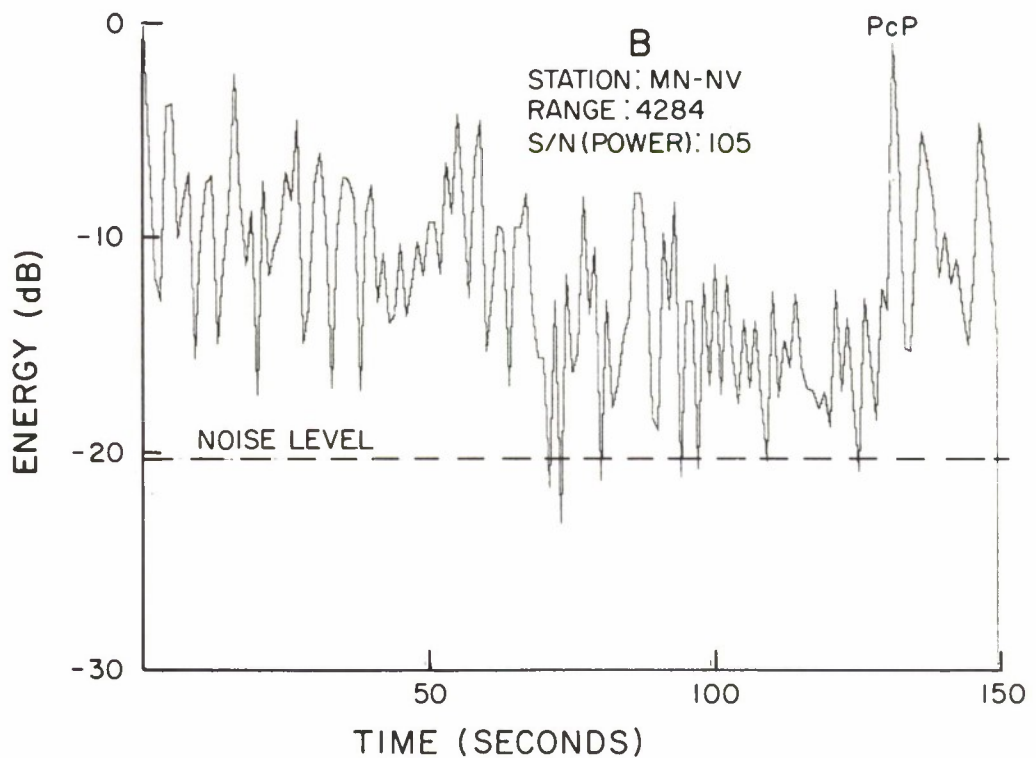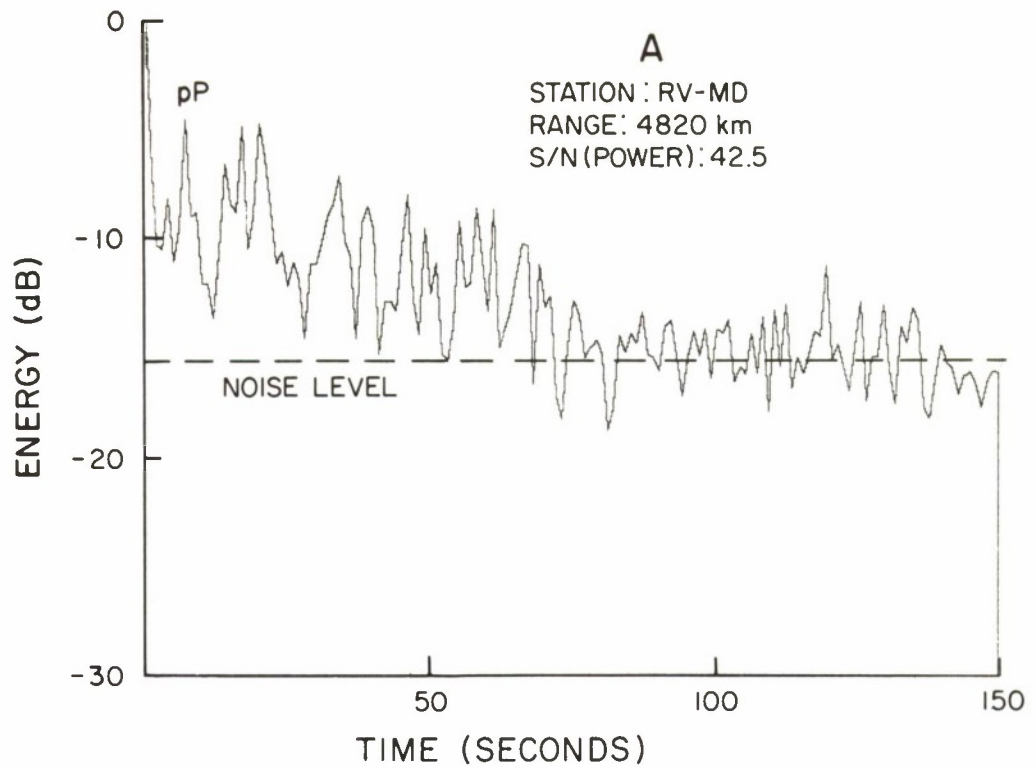
FIGURE 3.5 (A-B)
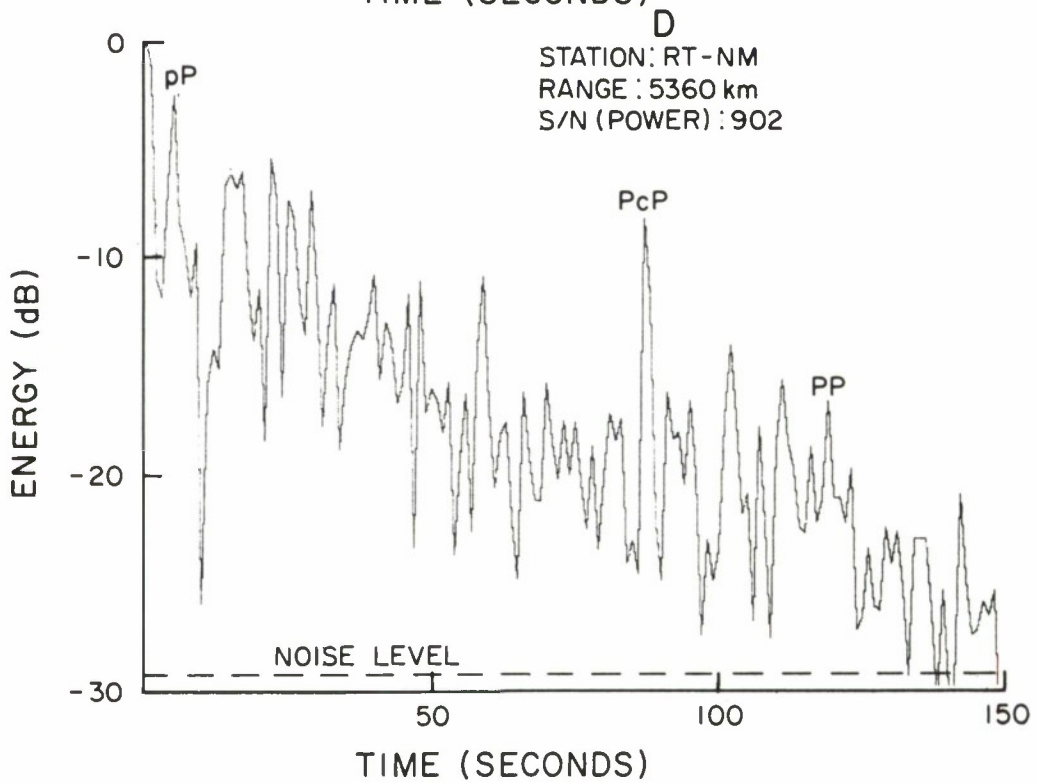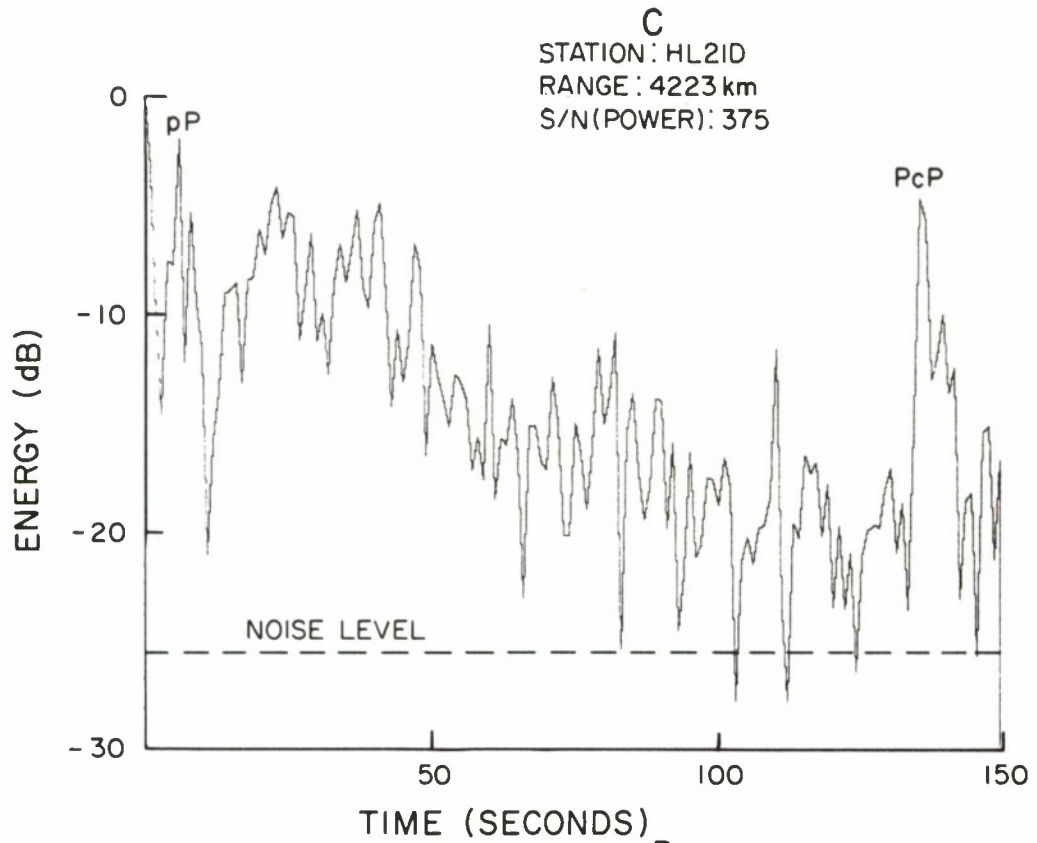ENERGY VS. TIME FOR SELECTED STATIONS (1 SEPT 64 EVENT)

FIGURE 3.5 (C-D)
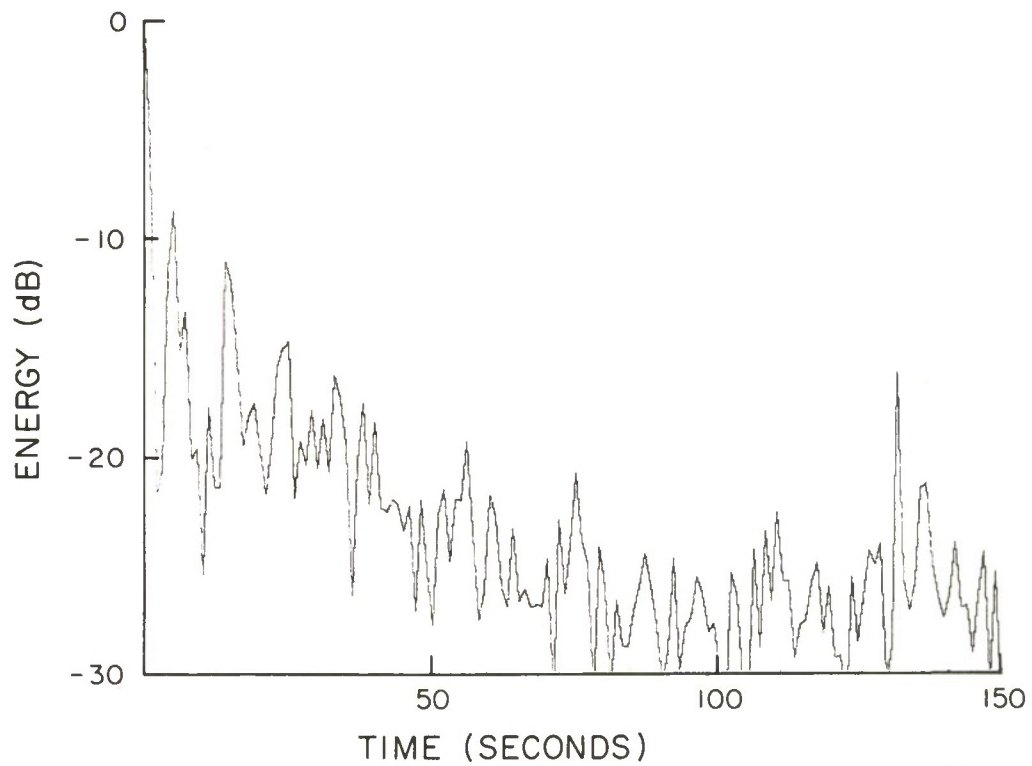ENERGY VS. TIME FOR SELECTED STATIONS (1 SEPT 64 EVENT)

FIGURE 3.6
ENERGY VS. TIME FOR PHASED SUM (I SEPT 64 EVENT)

phase arrival at the stations at small ranges from the epicenter. In many of these seismograms the amplitude of the PcP phase is approximately the same as that of the P-phase.

3.3   SUMMARY AND CONCLUSIONS

The problem of detecting a covert underground nuclear test in the proximity of a large natural earthquake has been studied. A detection system consisting of several single-seismometer stations encircling the epicenter at fairly close range plus one or more continental-size arrays has been considered. Assuming that the underground test will not be concealed if its signal precedes that of the earthquake at any of the single seismometers, a minimum time delay to avoid detection may be calculated as a function of test-site location. One example of this calculation, based on an earthquake epicenter in Mongolia and existing seismic stations was presented above.

The constraints imposed by the set of single seismometer stations may be described as areas of possible concealment as a function of the delay time between the earthquake and the test. To search these areas, the use of very large aperture seismic arrays has been discussed. In an earlier report, calculated array patterns were presented for such arrays, and these indicated a beamwidth approximately one order of magnitude smaller than that of LASA-Montana. However, these array patterns apply only to the very early portion of the earthquake during which the signals at the various seismometers are highly correlated. If a set of single seismometers exists, the period of a few seconds following the earthquake can be effectively monitored by these stations in the manner discussed above. Therefore, providing an adequate set of single stations exists, the calculated narrow beamwidth of the continental-size array is not of much interest insofar as detection is concerned. (Presumably, it would be very useful for location purposes.) The value of the array results from the uncorrelated contribution of coda at each station. Because the coda becomes decorrelated, the energy decays more rapidly in the array output than in the single seismogram. For this reason, the array would be significantly more sensitive than the individual seismometers. Furthermore, as long as the coda remains decorrelated, the sensitivity of the array would increase with increasing numbers of stations.

The energy decay curves presented above give some indication of the parameters of the detection problem. To date only a few impulsive earthquakes have been used, because they are easier to characterize than emergent ones. If a more quantitative analysis of this problem were desired, a larger number of events,including emergent ones, would, of course, have to be

processed. The calculated energy decay curve for the arrays assumes that the array is steered to the earthquake epicenter. Once the coda signal becomes decorrelated, it does not matter where the array is steered. For this reason, the curves also characterize the general form of energy decay for any steering of the array, except in the first few seconds.

We have observed that the directional characteristics of the array are not of value for the detection problem, since they do not apply to the time region of interest. The question thus arises as to the possibility of using a smaller array, such as the existing LASA-Montana. In a sense, the searching of possible areas of concealment would be easier since the wider beamwidth covers a larger fraction of the area. In addition, it would be appreciably easier to operate and process data with a LASA than with a continental-size array.

The difficulty with using an array with an aperture of LASA dimensions is that the earthquake coda will be more correlated between seismometers than it is with a continental-size array. This will reduce the sensitivity of the array. How serious this degradation in performance would be is not clear at the present time, since the data are not yet readily available that would allow calculation of energy decay curves of the kind presented above. Although some calculations exist of the coda correlation across LASA (and larger arrays) [9], in general these calculations cover only as far as 15 (not 150) seconds after the onset, and therefore are not sufficient.

The vast majority of this discussion has been rather qualitative: the structure of a possible detection system has been discussed, but absolute sensitivities for this or other systems have not been calculated. Additional work could lead to a more thorough understanding of this problem -- e.g., the minimum useful separation between array elements, the characterization of emergent events, and the consistency of energy decay data across a larger population of events. However, it is probably not appropriate to pursue too many quantitative details concerning the relative magnitudes and delay times necessary for an underground nuclear test to avoid risking detection. The reason for this is simply that large margins of error would have to be allowed in planning a covert underground test since precise earthquake prediction is not possible. To illustrate some of the parameters of the problem, there were approximately 100 seismic events in the Sino-Soviet bloc between March 1966 and March 1967 with magnitudes of 5.0 or larger (according to C&GS PDE cards). Of these 100 events, only five were earthquakes larger than 6.0 in magnitude.

SECTION IV

DIMUS ARRAY PROCESSING

4.1   INTRODUCTION

This section of the report covers further investigations of the use of DIMUS array processing for a seismic detection and classification network. Prior work [10] discussed the advantages of DIMUS processing, and also demonstrated that the detection capability of an array which used DIMUS processing would be negligibly affected as compared with an array which used analog processing. The major concern is the loss in signal fidelity which DIMUS introduces, and the consequent effect on the ability of a DIMUS array to classify seismic signals. The work done during this period has been concerned solely with the classification capability of DIMUS-type arrays.

Let us recall that in DIMUS processing each seismometer output is hardlimited, and the outputs of the individual hardlimiters are appropriately delayed, and then the delayed signals are summed to form a beam. Thus, in the case of N seismometers the maximum positive array output is N, and the maximum negative array output is -N.

Certain rough generalizations can be made about signal fidelity and DIMUS processing. First, there is excellent agreement in the location of zero crossings of the DIMUS array output when compared with an equivalent analog array. Second, when the instantaneous input signal-to-noise ratio to the DIMUS array is high, the output of the DIMUS array tends to underestimate the true value of the signal. And thirdly, when the instantaneous input signal-to-noise ratio to the DIMUS array is low, the output of the DIMUS array tends to overestimate the true value of the signal. Figure 4.1 demonstrates all of the above effects. Figure 4.1 shows the output of a 21-element DIMUS array formed from the center elements of the LASA clusters, and the corresponding output of the analog array. The seismic event shown is a magnitude 5 underground explosion.

The underestimation of signal at high signal-to-noise ratios is caused by saturation effects in DIMUS. That is, as the input signal-to-noise ratio to the DIMUS array increases, the array output increases until a value of N is reached. Any further increase in signal-to-noise ratio will not cause any further increase in array output. Thus, at high signal-to-noise ratios, DIMUS slices off the tops of the signal peaks and introduces severe distortion in the region of high signal peaks. Even when the signal-to-noise ratio is not large enough to cause the DIMUS array to reach a value of N, it is found that DIMUS

-33-

UNDERGROUND EXPLOSION
MAGNITUDE 5.0

ANALOG BEAM (UNFILTERED)
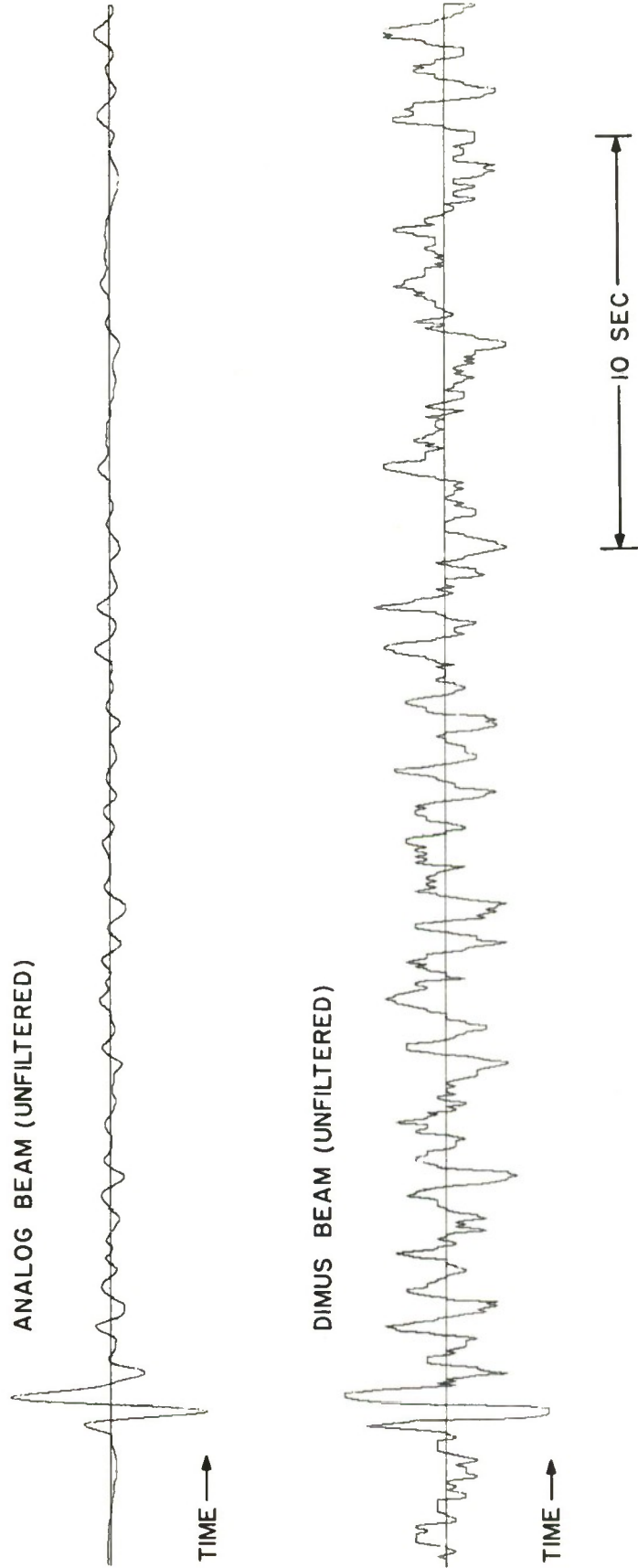
DIMUS BEAM (UNFILTERED)

TIME ⟶

TIME ⟶

10 SEC

FIGURE 4.1

COMPARISON OF ANALOG AND DIMUS PROCESSING

underestimates the true signal value for moderately high signal-to-noise ratios. The overestimation of the signal at low signal-to-noise ratio is due to the fact that quantization noise dominates the output of the DIMUS array.

It is evident from Figure 4.1 that DIMUS processing introduces significant signal distortion, and hence it can be expected that the classification capability will be impaired. Thus we must seek ways to modify the output of the DIMUS array. Bandpass filtering of the DIMUS array output will improve the situation by reducing the amount of quantization noise, and eliminating the out-of-band modulation products introduced by the limiting process. However, in many cases, filtering alone was not found to improve the fidelity of the DIMUS output sufficiently for adequate classification. Based on the observation that DIMUS preserves zero crossings and that the severest signal distortion occurred at regions of high instantaneous signal-to-noise ratio it was felt that the analog output of a single seismometer could be used to modify the DIMUS output in order to improve signal fidelity. Basically, the technique involves replacing the DIMUS output with a scaled version of the single analog channel whenever the DIMUS output achieves a value of N, and then bandpass filtering the output. This report considers several methods of utilizing the single analog channel as a modifier. Figure 4.2 shows the transfer characteristic of the bandpass filter that was used to filter the output of the modified DIMUS array.

4.2   DIMUS MODIFICATIONS

A simple DIMUS modification was briefly discussed in a previous report [11]. This modification was obtained in the following manner. At the first point in time when the DIMUS output achieves a value $\pm N$, the corresponding value of the single analog channel is noted. Let the analog channel output at this time be called V_L. The analog channel is then adjusted so that its value at the noted point is equal to N. The remaining portion of the analog output is scaled by a factor N/V_L. Now, the value of DIMUS output is retained as long as it has a value less than N. However, when its value reaches N, its value is replaced by the corresponding value of the scaled analog channel. The modified result is then bandpass filtered using the filter of Figure 4.2.

Some thought was given to the possibility of modifying the DIMUS output with single analog channel when the DIMUS output reached a value lower than $\pm N$, say $\pm(N-2)$. This possibility was quickly discarded for the following reason. At any time when the DIMUS output does not completely saturate at a value $\pm N$, there will be at least one channel which is of opposite phase with respect to the majority of the other channels.
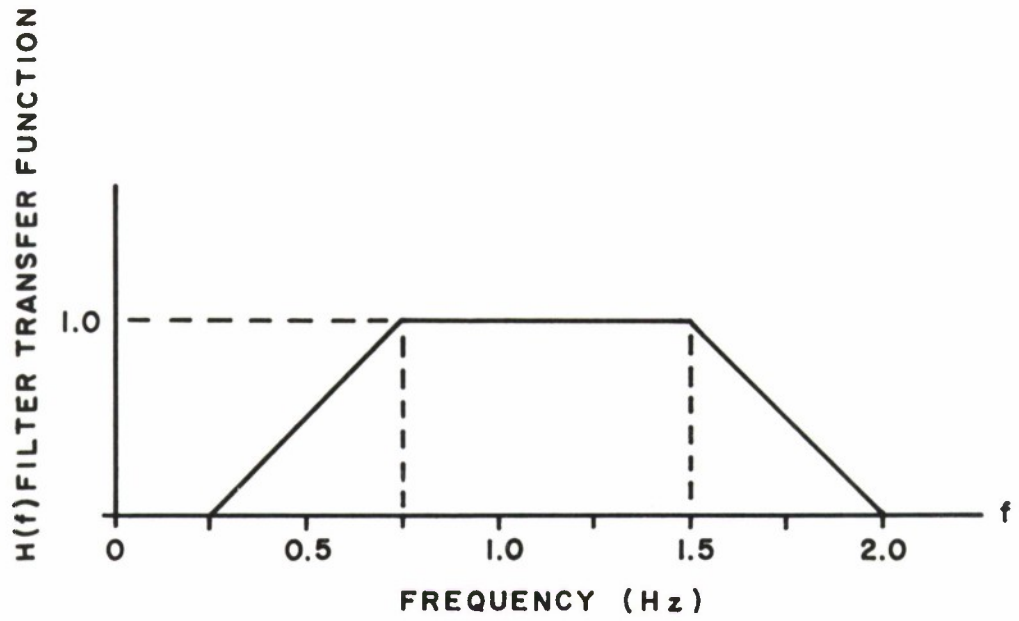
FIGURE 4.2
BANDPASS FILTER TRANSFER CHARACTERISTIC

The possibility exists that the single analog channel used for modification may be the out-of-phase channel. Thus, if modification is allowed to occur at DIMUS levels less than N, the danger exists that the analog channel used for modification may be out of phase with respect to the DIMUS sum, in which case the modification will cause a drastic distortion in the modified waveform.

In the previous work the above modification was applied to a single seismic event. The modification was found to yield an output waveform whose signal fidelity was superior to the filtered output of an ordinary DIMUS array using the filtered output of an equivalent analog array as a comparison. One of the first steps in the present DIMUS studies was to apply this DIMUS modification to a more extensive collection of seismic events. One difficulty was observed when the modification was applied to a wider class of events. This difficulty arises whenever the DIMUS output saturates during more than one time interval over the duration of the seismic event. The modification requires that the DIMUS output be replaced by the scaled version of the single analog channel over each of these saturated regions. Thus, unless the single analog channel has identical amplitudes at the time instants when the DIMUS output enters and leaves saturation, a step discontinuity will be introduced at each such point whenever the single analog channel differs in amplitude from V_L. These step discontinuities are a source of distortion in the output waveform. To eliminate these possible discontinuities the original DIMUS modification was altered slightly. Instead of scaling the analog channel by a single factor N/V_L, a different scale factor is used over each saturation interval. The scaling factor used over the i-th saturation interval is N/V_{Li}, where V_{Li} is the amplitude of the analog channel at the instant of time when the DIMUS output just enters the i-th saturation interval. Thus over the i-th saturation interval the DIMUS output is replaced by the analog channel scaled by a factor N/V_{Li}. Thus, there are no discontinuities introduced by this revised modification at the start of each saturation interval. There may still exist slight discontinuities as the DIMUS output comes out of saturation. But these discontinuties will, in general, be small. As before, the modified DIMUS output is bandpass-filtered. In the following, this revised DIMUS modification will be referred to as MOD-DIMUS 1.

Twenty-one seismic events were examined using the MOD-DIMUS 1 modification. The array utilized the 21 center elements of the LASA clusters. Figures 4.3 through 4.7 illustrate some of the results that were obtained. Each of these figures contains three output traces; the top trace corresponds to the output of a 21-element analog array, the middle trace corresponds

to the output of a 21-element DIMUS array, and the bottom trace
to a 21-element array utilizing the MOD-DIMUS 1 modification.
In each case the array output was filtered using the filter of
Figure 4.2.

Figure 4.3 corresponds to a magnitude 6 underground
explosion. As can be seen the DIMUS output is severely distorted.
The DIMUS modification reduces the amount of distortion. However,
the first few seconds of the main arrival still remains heavily
distorted. Figure 4.4 corresponds to a magnitude 4.5 earthquake.
The amount of distortion introduced by DIMUS is not too severe
since the signal-to-noise ratio is only moderately high. The
main distortion introduced by DIMUS for this case is the magni-
fication of the low-level coda. The DIMUS modification yields a
slight improvement compared with DIMUS in that the coda levels
have been reduced somewhat. Figure 4.5 corresponds to a magni-
tude 6.2 underground explosion, Figure 4.6 to a magnitude 5.8
underground explosion, and Figure 4.7 to a magnitude 6.3 under-
ground explosion. In each of these cases DIMUS overemphasizes
the low level coda, whereas the DIMUS modification restores
the proper relation between the amplitude of the main arrival
and the general amplitude level of the low-level coda. Both
DIMUS and the DIMUS modification yield distorted main arrivals
over the first few seconds of the seismogram.

In general, it was observed that the DIMUS modification
yielded a better relation between the amplitude level of the
main arrivals and the amplitude level of the coda when compared
to DIMUS. However, the DIMUS modification tended to distort
the main arrival more severely than did DIMUS. This distortion
was such that the portion of the signal corresponding to the
half-cycle of first motion was magnified out of proportion with
respect to the rest of the trace. This effect of magnification
of the first motion by the DIMUS modification is clearly shown
in Figure 4.8 which corresponds to a magnitude 5.6 underground
explosion.

The reason why the MOD-DIMUS 1 modification magnifies
the first motion is evident when one considers how delay times
for beam-formation were chosen and the method of scaling used
in the modification. The individual analog seismogram traces
are examined and the first zero-crossing after what is thought
to be first motion is picked out by eye, and then the individual
seismograms are brought into time alignment with respect to these
zero-crossings in order to form a beam. Thus it is highly likely
that because of this time alignment all twenty-one seismogram
traces will have the same polarity over most of the half-cycle
corresponding to "first motion." Hence, for most cases the DIMUS
output saturates over most of the half-cycle corresponding to
first motion. Furthermore, the onset of saturation will usually
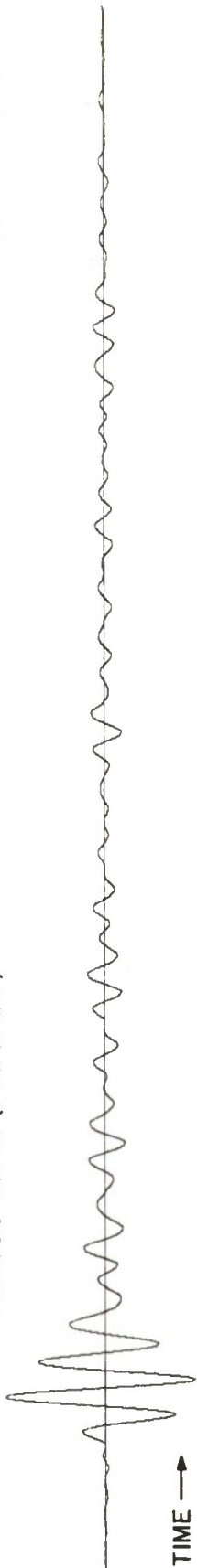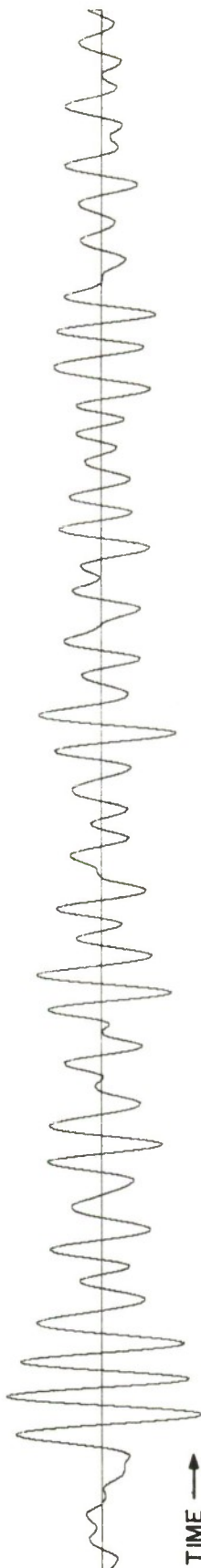
EARTHQUAKE
DEPTH: 33 KM
MAGNITUDE 4.5

ANALOG BEAM (FILTERED)

TIME →

DIMUS BEAM (FILTERED)

TIME →

MOD-DIMUS I (FILTERED)

TIME →
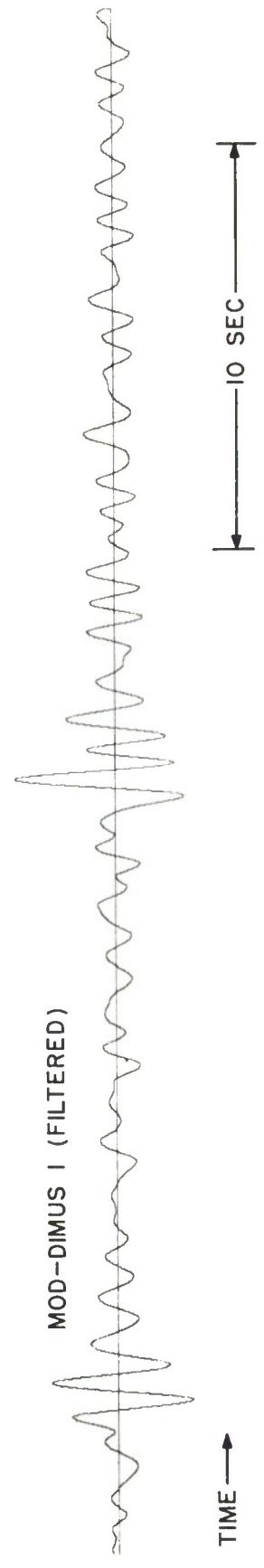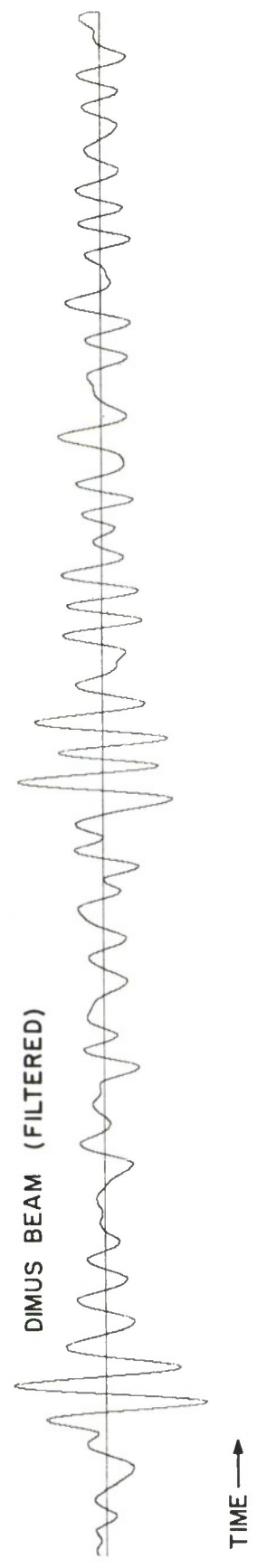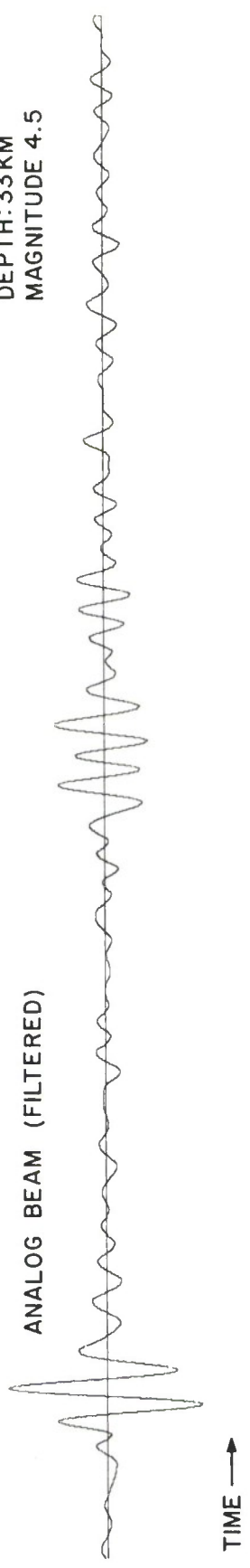
10 SEC

FIGURE 4.4
MOD-DIMUS I MODIFICATION

UNDERGROUND EXPLOSION
MAGNITUDE 6.0

ANALOG BEAM (FILTERED)

TIME →

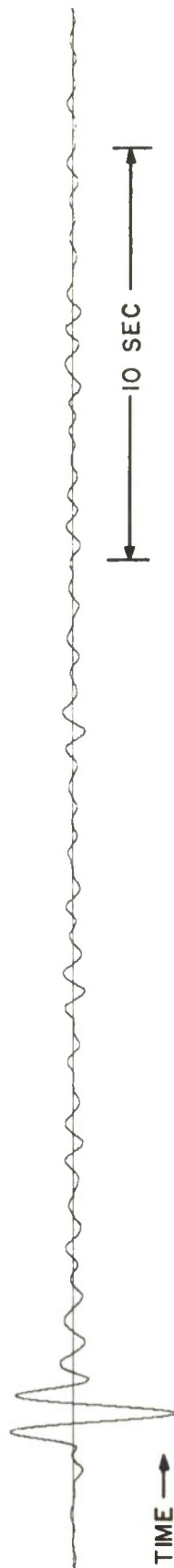DIMUS BEAM (FILTERED)

TIME →

MOD-DIMUS I (FILTERED)

TIME →

10 SEC

FIGURE 4.3
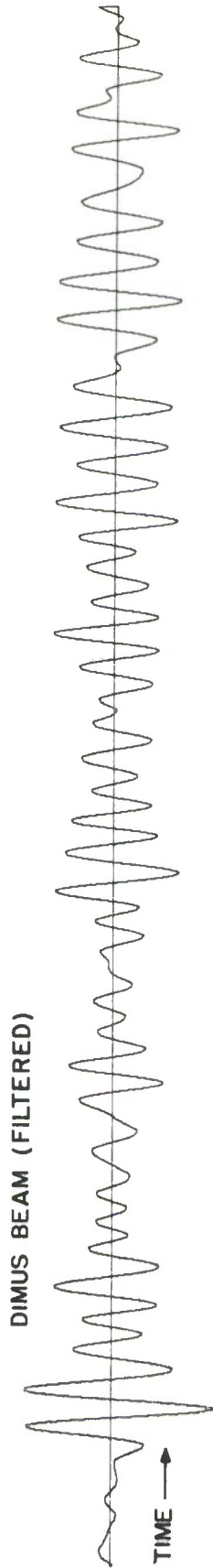MOD-DIMUS I MODIFICATION

UNDERGROUND EXPLOSION
MAGNITUDE 6.2

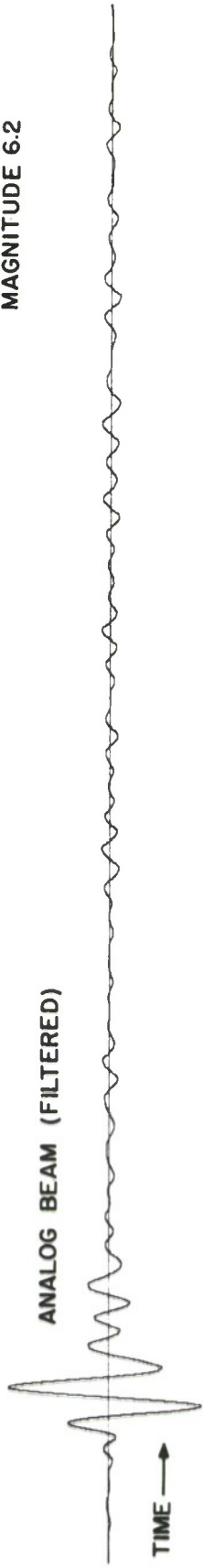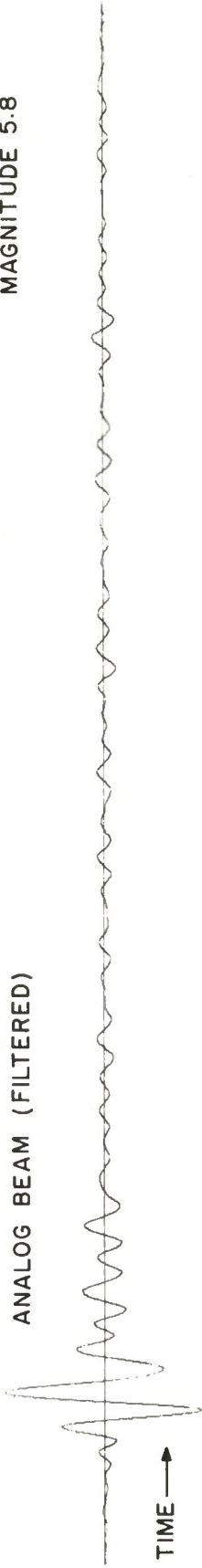ANALOG BEAM (FILTERED)

TIME ——▶

DIMUS BEAM (FILTERED)

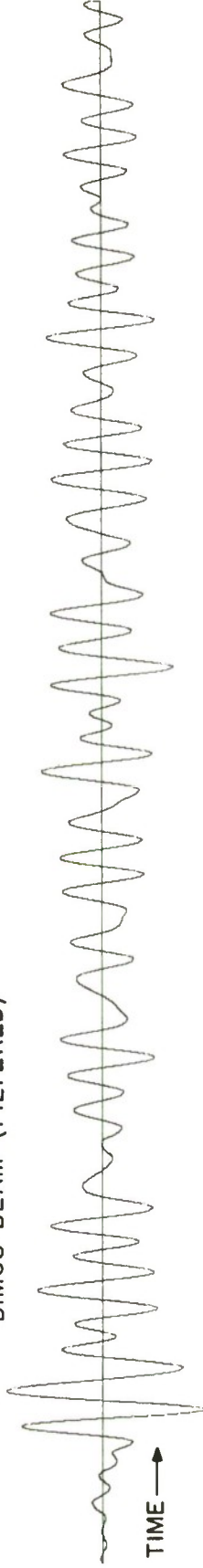TIME ——▶

MOD-DIMUS I (FILTERED)

TIME ——▶

|◀— 10 SEC —▶|
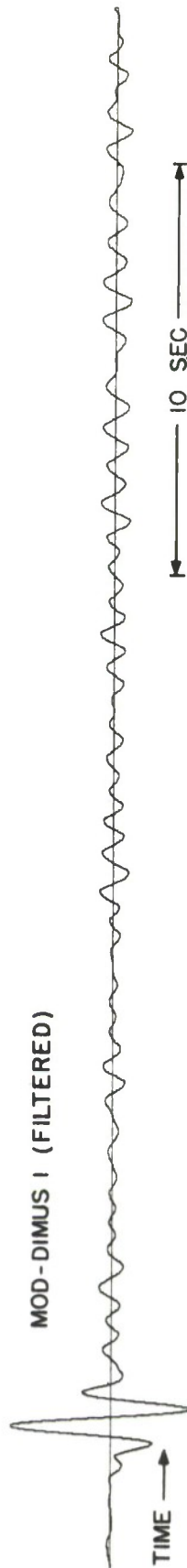
FIGURE 4.5
MOD-DIMUS I MODIFICATION

-41-

UNDERGROUND EXPLOSION
MAGNITUDE 5.8

ANALOG BEAM (FILTERED)

TIME →

DIMUS BEAM (FILTERED)

TIME →

MOD-DIMUS I (FILTERED)

TIME →

10 SEC

FIGURE 4.6
MOD-DIMUS I MODIFICATION

UNDERGROUND EXPLOSION
MAGNITUDE 6.3

ANALOG BEAM (FILTERED)

TIME →

DIMUS BEAM (FILTERED)

TIME →

MOD-DIMUS I (FILTERED)
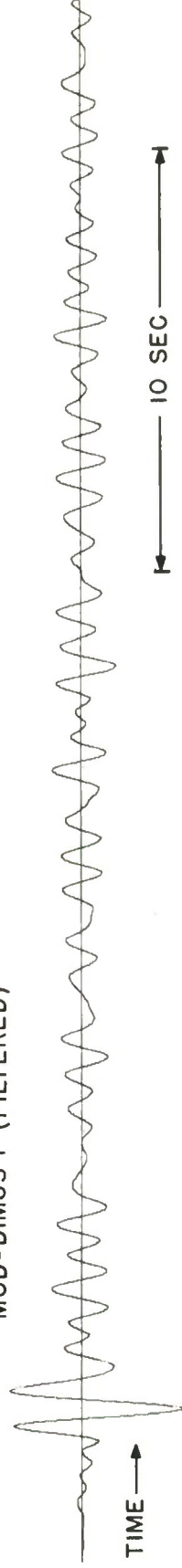
TIME →

10 SEC

FIGURE 4.7
MOD-DIMUS I MODIFICATION

-43-

UNDERGROUND EXPLOSION
MAGNITUDE 5.6

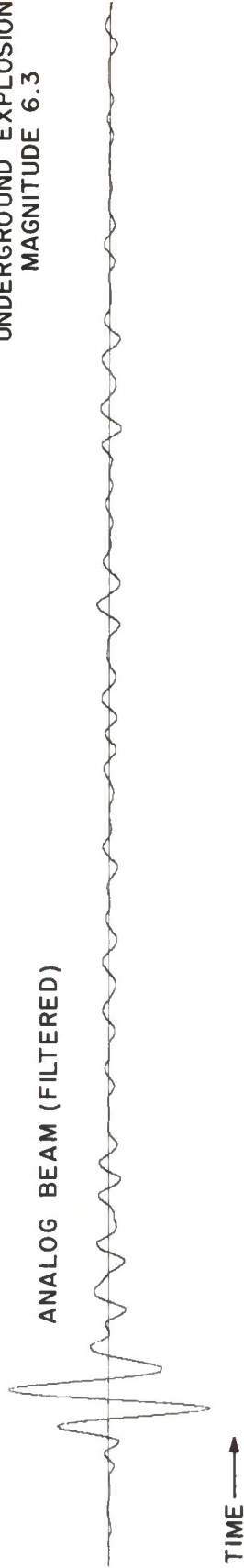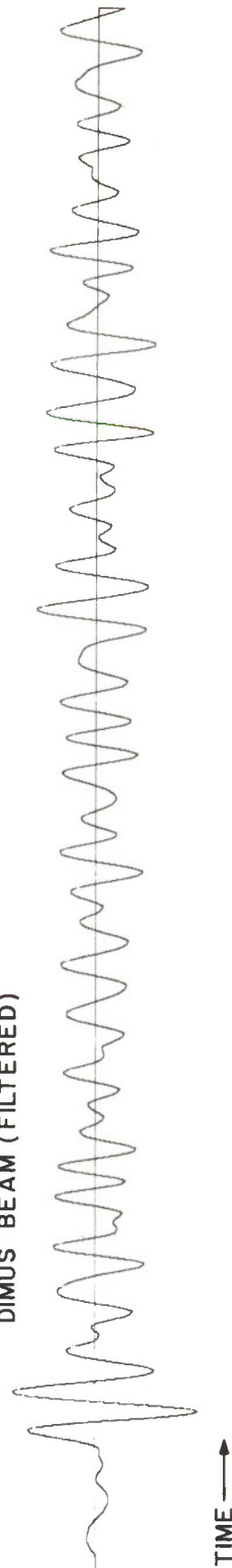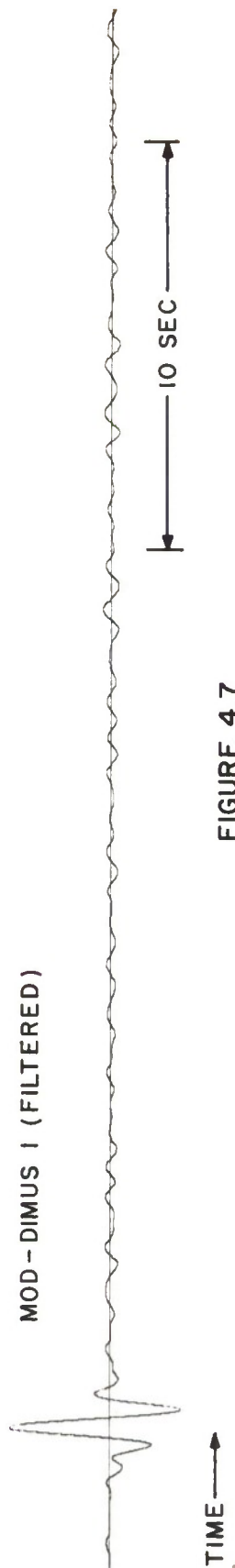ANALOG BEAM (FILTERED)

DIMUS BEAM (FILTERED)
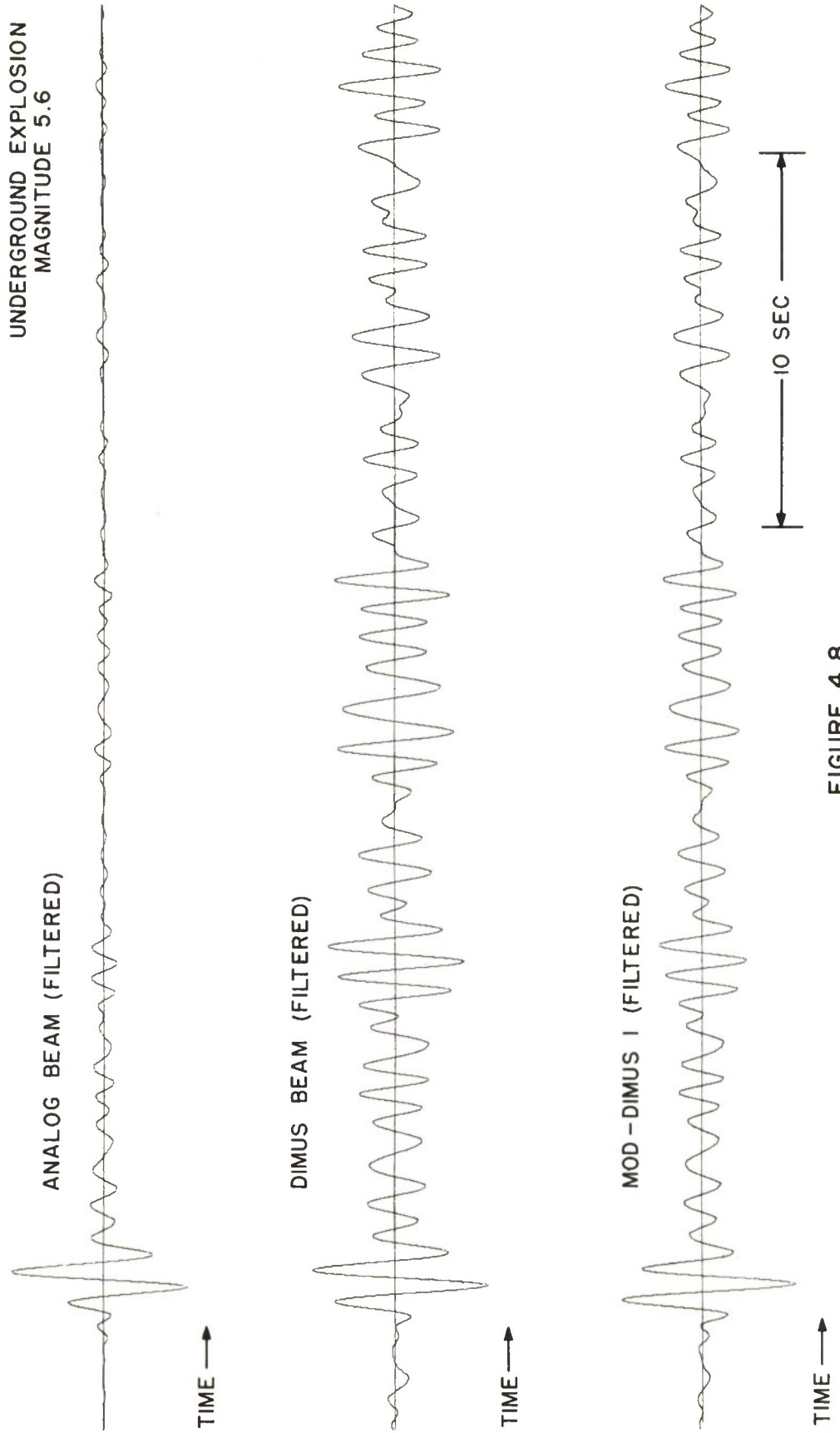
MOD-DIMUS I (FILTERED)

TIME

TIME

TIME

10 SEC

FIGURE 4.8
MOD-DIMUS I MODIFICATION

-44-

occur at a very low ampltiude level and hence the scale factor $21/V_{L1}$ will be quite large. The quantity V_{L1} is the amplitude level of the single seismogram trace (which is used for modification) at the point at which the DIMUS output first saturates during first motion. At other portions of the seismogram trace where saturation of DIMUS takes place, the onset of saturation will occur at an amplitude level V_{Li} which, in general, is higher than V_{L1}. This is due to the fact that as one proceeds away from the point of time alignment the individual seismogram traces slip out of phase. Hence the scale factors $21/V_{Li}$ for other regions of saturation are generally smaller than $21/V_{L1}$. Hence the MOD-DIMUS 1 modification tends to magnify first motion.

The distortion introduced by the magnification of first motion is undesirable and hence it was necessary to seek another method of modifying the DIMUS output. It was felt that an improved modification could be obtained if the envelope of the single analog channel could be used to further correct the modified DIMUS output. Such a correction would tend to bring various portions of the output trace into proper proportion.

This reasoning led to a new DIMUS modification which will now be described. First, the MOD-DIMUS 1 output (prior to filtering) was taken, and each half-cycle over which saturation occurred was rescaled so that the peak value within the half-cycle had a value of 21. No rescaling was done in those half-cycles where saturation failed to occur. Next, the single analog channel output (used for correction) was taken and an average value was obtained for the magnitudes of each set of sample points between each set of zero-crossings of the analog channel. Now corresponding sample points on the rescaled MOD-DIMUS 1 output are multiplied (sample point by sample point) by the above computed average values such that all modified DIMUS sample points which fall within a given interval between zero-crossings on the single analog channel are multiplied by the average value computed for that zero-crossing interval. This last correction essentially provides the desired scaling according to the envelope of the single analog channel. This final corrected output is then filtered by the filter of Figure 4.2. This new DIMUS modification will be referred to as MOD-DIMUS 2.

The MOD-DIMUS 2 modification was applied to the previous 21 seismic events used to study the MOD-DIMUS 1 modification, plus three additional events. For each of the events studied the MOD-DIMUS 2 modification was found to yield a less distorted signal when compared with the MOD-DIMUS 1 modification. Figures 4.9 through 4.14 show the results for the MOD-DIMUS 2 modification. The seismic events used correspond to the same events shown in Figures 4.3 through 4.8 for the MOD-DIMUS 1 modification. Comparison of Figure 4.4 and 4.10 (a magnitude 4.5 earthquake) shows
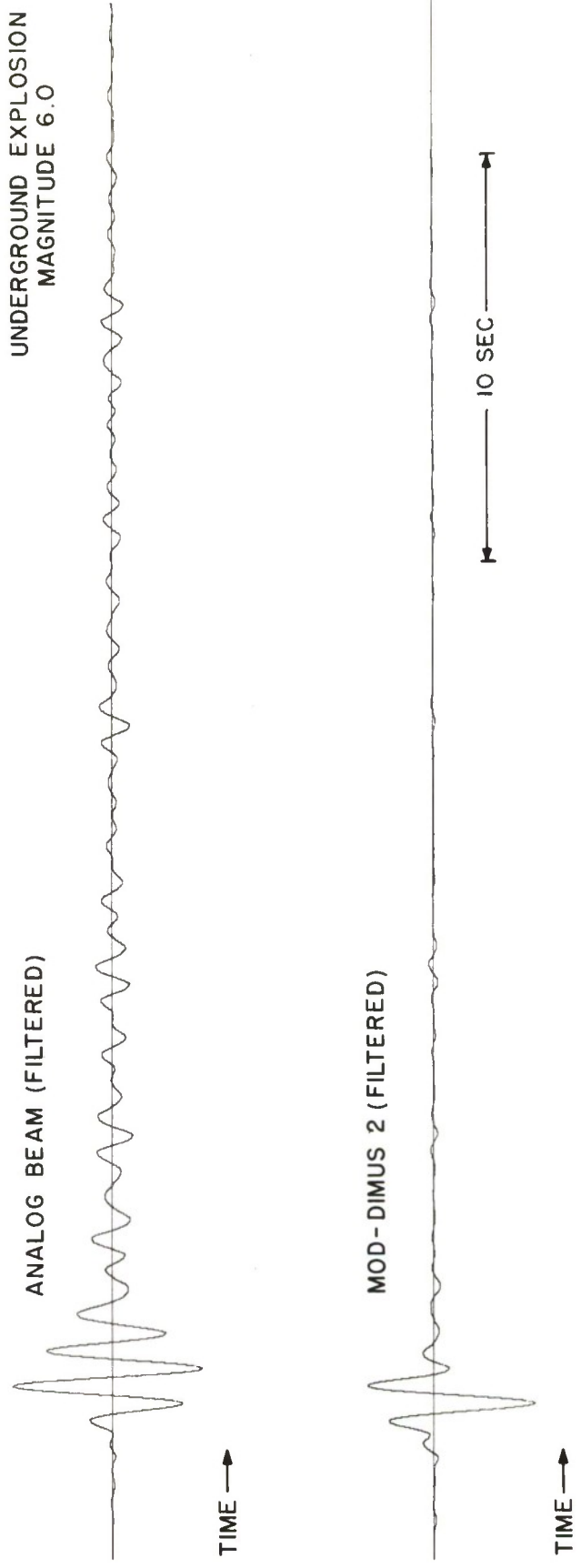
UNDERGROUND EXPLOSION
MAGNITUDE 6.0

ANALOG BEAM (FILTERED)

TIME ⟶

MOD-DIMUS 2 (FILTERED)

TIME ⟶

10 SEC

FIGURE 4.9
MOD-DIMUS 2 MODIFICATION

EARTHQUAKE
DEPTH:33 KM
MAGNITUDE 4.5

ANALOG BEAM (FILTERED)

TIME ——►

MOD-DIMUS 2 (FILTERED)

TIME ——►

IO SEC
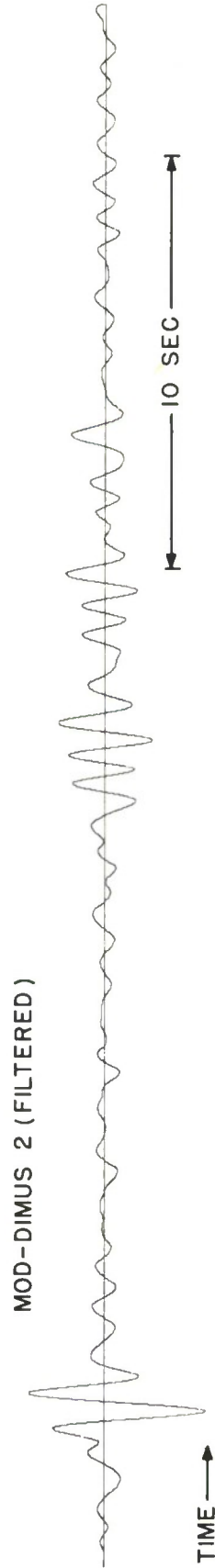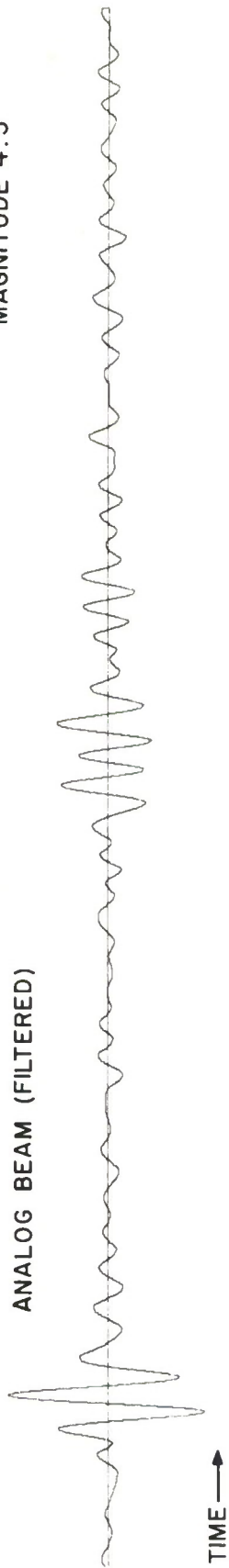
FIGURE 4.10
MOD-DIMUS 2 MODIFICATION

UNDERGROUND EXPLOSION
MAGNITUDE 6.2

ANALOG BEAM (FILTERED)

MOD-DIMUS 2 (FILTERED)

TIME ⟶

TIME ⟶

10 SEC
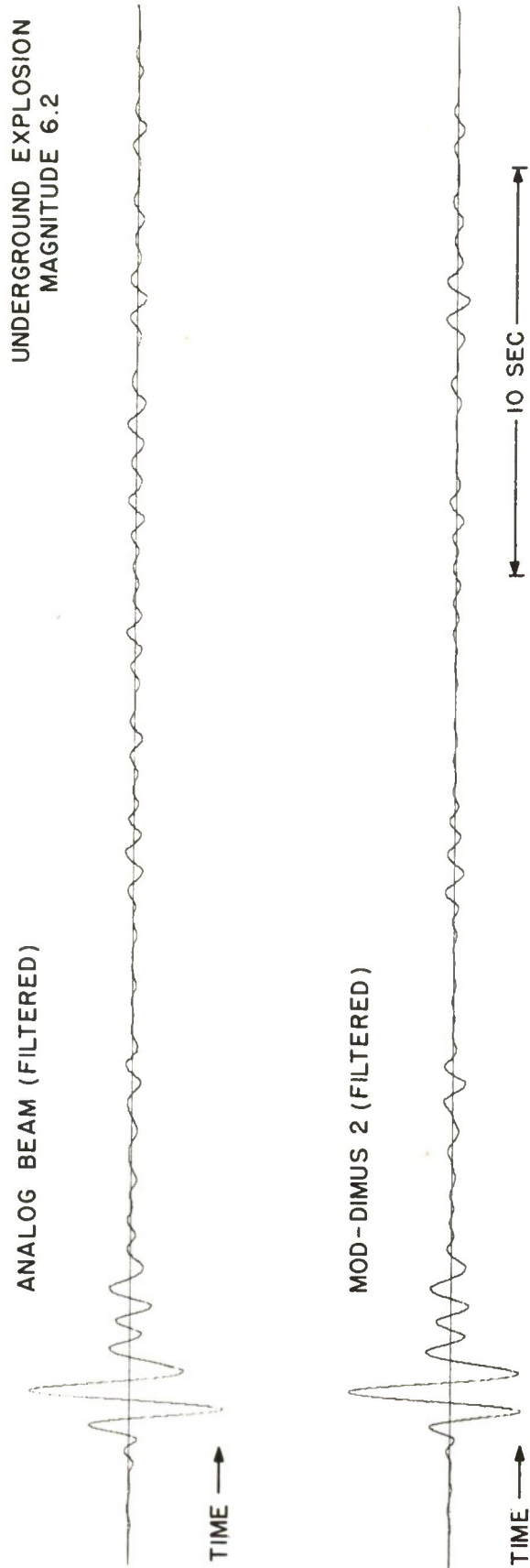
FIGURE 4.11
MOD-DIMUS 2 MODIFICATION

UNDERGROUND EXPLOSION
MAGNITUDE 5.8

ANALOG BEAM (FILTERED)

TIME

MOD-DIMUS 2 (FILTERED)

TIME

10 SEC
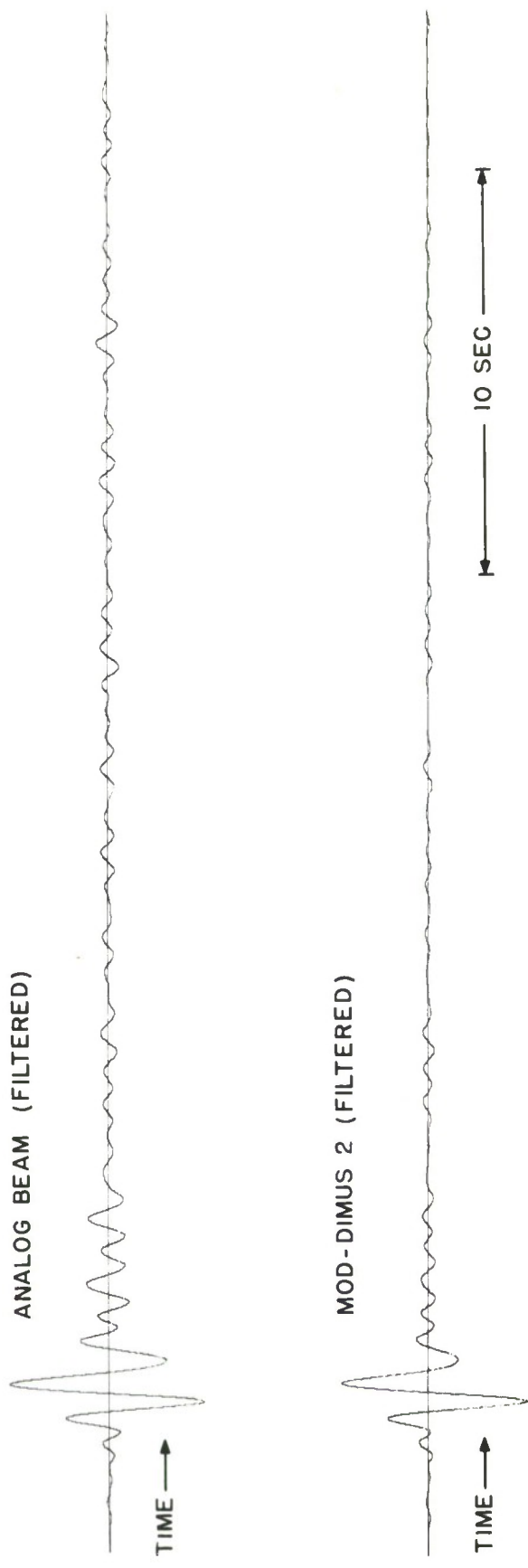
FIGURE 4.12
MOD-DIMUS 2 MODIFICATION

UNDERGROUND EXPLOSION
MAGNITUDE 6.3

ANALOG BEAM (FILTERED)

TIME →

MOD-DIMUS 2 (FILTERED)

TIME →

10 SEC
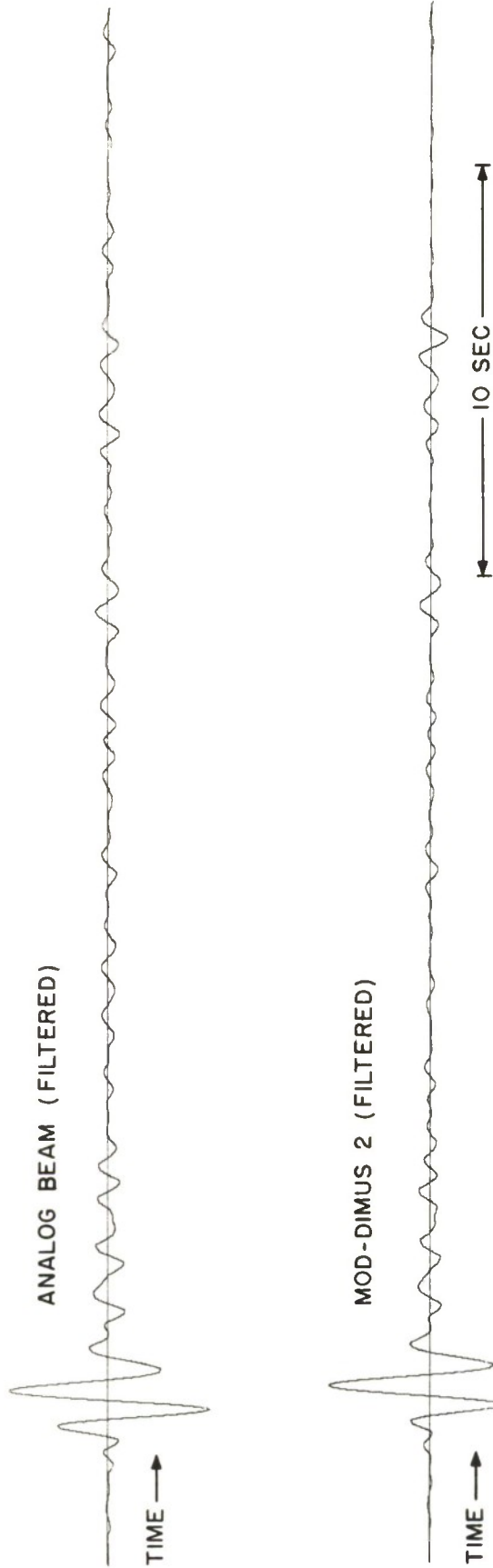
FIGURE 4.13
MOD-DIMUS 2 MODIFICATION

UNDERGROUND EXPLOSION
MAGNITUDE 5.6

ANALOG BEAM (FILTERED)

MOD-DIMUS 2 (FILTERED)
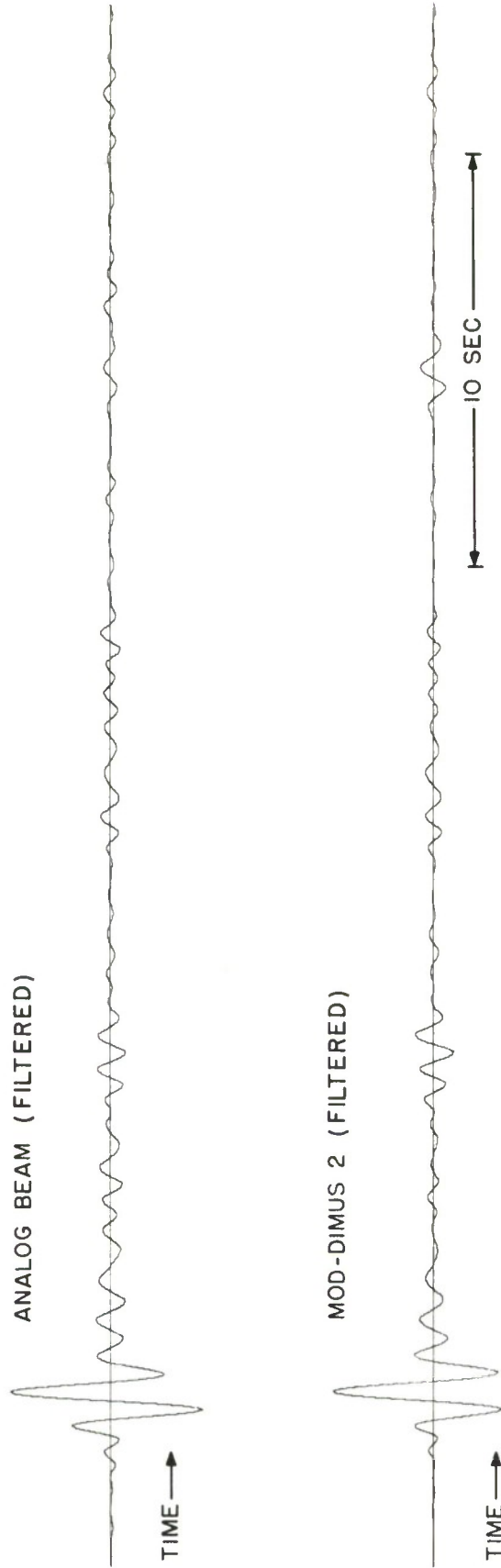
TIME

TIME

10 SEC

FIGURE 4.14
MOD-DIMUS 2 MODIFICATION

that the new DIMUS modification yields a significantly less distorted waveform. In particular, the shape of pP is greatly improved and its amplitude is in the proper proportion to main P. Figure 4.11 (a magnitude 6 underground explosion) shows that the new modification has lessened the amount of signal distortion. However, the general shape of the main arrival still leaves something to be desired. In general, it was found that the MOD-DIMUS 2 modification yielded an output waveform which closely resembled the waveform obtained from the analog array in about 50% of the cases examined. In the remaining cases, although signal distortion was lessened compared with the MOD-DIMUS 1 modification, there were still portions of the corrected waveform which were obviously distorted when compared to the waveform obtained from the analog array.

4.3   DISCRIMINANT ANALYSIS

The above discussion of the amount of signal distortion introduced by DIMUS and the various DIMUS modifications has been quite qualitative. To obtain some quantitative measure of the distortion introduced by DIMUS-type processors, two diagnostics were applied to the outputs of the analog array, the DIMUS array, the MOD-DIMUS 1 array, and the MOD-DIMUS 2 array. The diagnostics chosen were the complexity ratio criterion, and the spectral ratio criterion.

The complexity ratio is defined as [12]

$$C = \frac{\int_{5}^{30} |f(t)| dt}{\int_{0}^{5} |f(t)| dt}$$

where $f(t)$ is the output waveform, and t is time in seconds. The spectral energy ratio S_E is defined as

$$S_E = \frac{\int |F(f)|^2 |H_1(f)|^2 df}{\int |F(f)|^2 |H_2(f)|^2 df}$$

where $F(f)$ is the Fourier transform of the output waveform $f(t)$, and $H_1(f)$ and $H_2(f)$ are filter transfer characteristics. $H_1(f)$ is centered in a low frequency band, and $H_2(f)$ is centered in a band of frequencies above $H_1(f)$. For the present study H_1 and H_2 were chosen as 3-pole Butterworth filters, with H_1 covering the band of frequencies from 0.3 to 0.7 Hz, and H_2 covering the band of frequencies from 1.5 to 1.9 Hz. Also it should be noted that in the spectral energy ratio test $f(t)$ was taken to have a length of 25 seconds. The above diagnostic tests

were applied to unfiltered versions of the analog array output, DIMUS array output, and the outputs of the two modified DIMUS arrays. That is, the bandpass filtering (Figure 4.2) was omitted.

Figure 4.15 shows the results of the complexity test as applied to the various processors for 24 seismic events. In the case of the MOD-DIMUS 1 processor only 21 events were used. Also shown in the figure is a horizontal partition line for each case. In each case, the best partition line was drawn based on the *a priori* knowledge of the nature of the event. Based on these thresholds, the following classification errors were obtained; 2 out of 24 for the analog array, 7 out of 24 for DIMUS, 6 out of 21 for MOD-DIMUS 1, and 2 out of 24 for MOD-DIMUS 2. Thus it is found that for the complexity test, the MOD-DIMUS 2 array performs as well as the analog array, and that the DIMUS and MOD-DIMUS 1 arrays performed only moderately poorer than the analog array.

To apply the spectral ratio test it is necessary first to plot the spectral ratio S_E versus the magnitude of the event for which it was calculated. Then the resulting plot is divided into two parts by a straight line. Points falling below the line are classified as earthquakes and points falling above the line are classified as explosions. Figures 4.16, 4.17, 4.18 and 4.19 show such plots, respectively, for the analog array, DIMUS array, MOD-DIMUS 1 array, and the MOD-DIMUS 2 array. Also included are a set of partition lines. As in the case of the complexity discriminant, the lines were drawn to provide the best separation between earthquakes and explosions based on the *a priori* knowledge of the nature of the events. Based on the above partitions, the following classification errors were obtained; 3 out of 24 for the analog array, 3 out of 24 for DIMUS, 3 out of 21 for MOD-DIMUS 1, and 7 out of 24 for MOD-DIMUS 2. In this case, both DIMUS and MOD-DIMUS 1 performed as well as the analog array whereas MOD-DIMUS 2 performed moderately poorer.

The above results on the effect of DIMUS processing on classification are still preliminary. However, based on the two diagnostics examined, it was found that for the seismic events examined, DIMUS-type processors do not significantly degrade classification performance when compared to the analog array. In fact, for each discriminant there was a DIMUS-type processor which did as well as the analog array.

During the next period it is planned to study further DIMUS-type processors and their effect on classification capability. An attempt will be made to see if an improved DIMUS modification can be obtained. In particular, an improved method
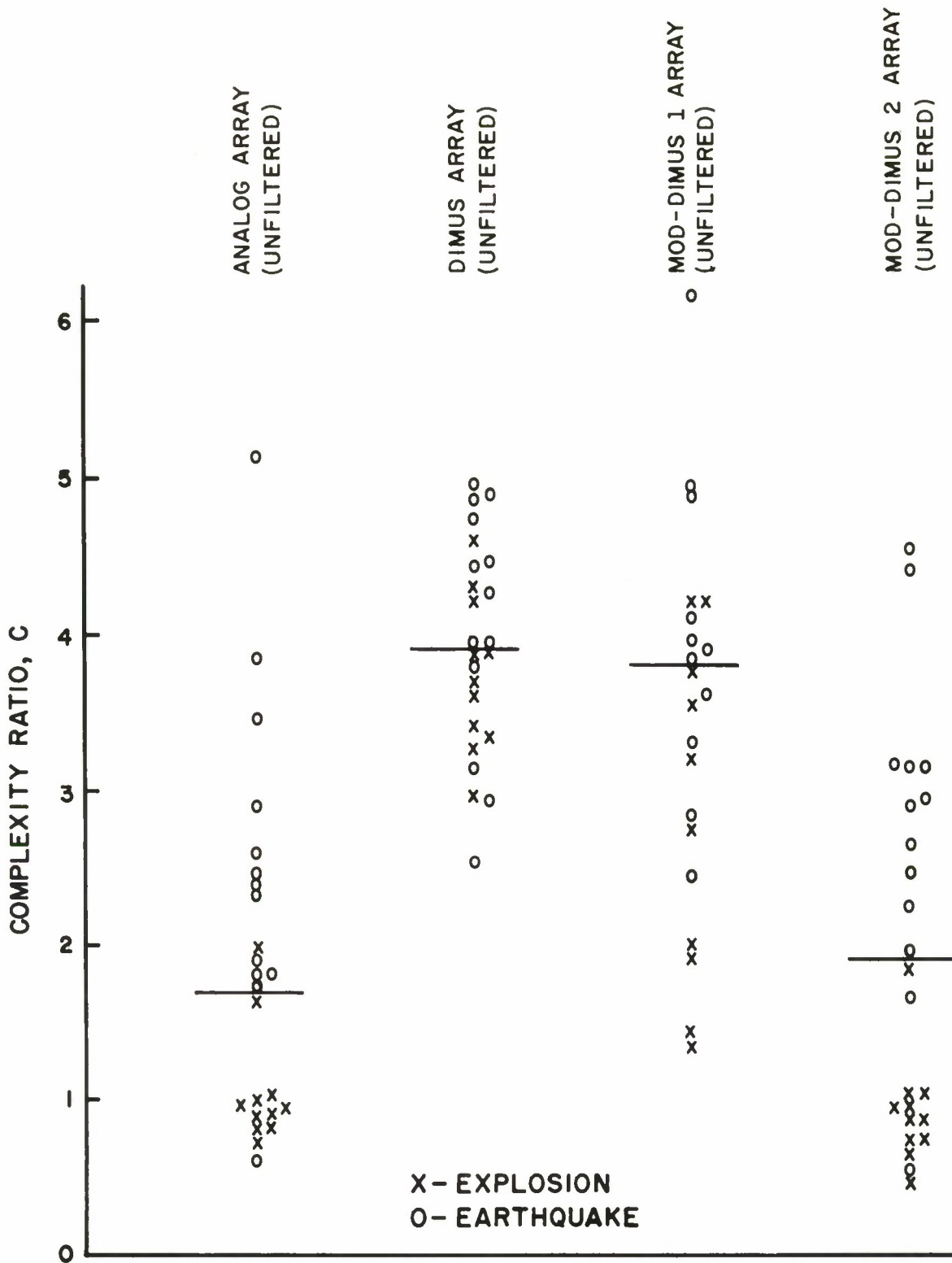
FIGURE 4.15
COMPLEXITY RATIO TEST

FIGURE 4.16
SPECTRAL ENERGY RATIO TEST
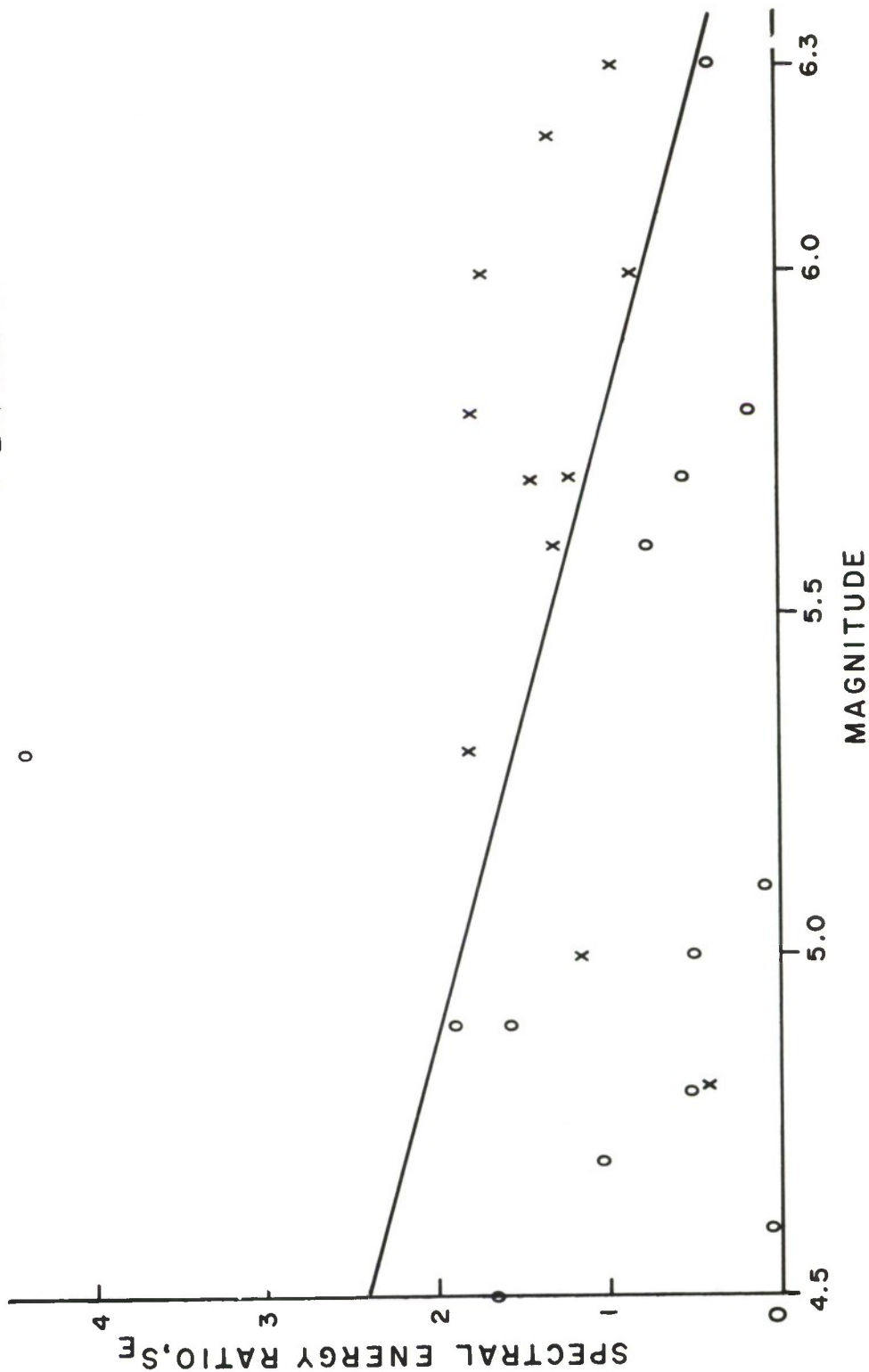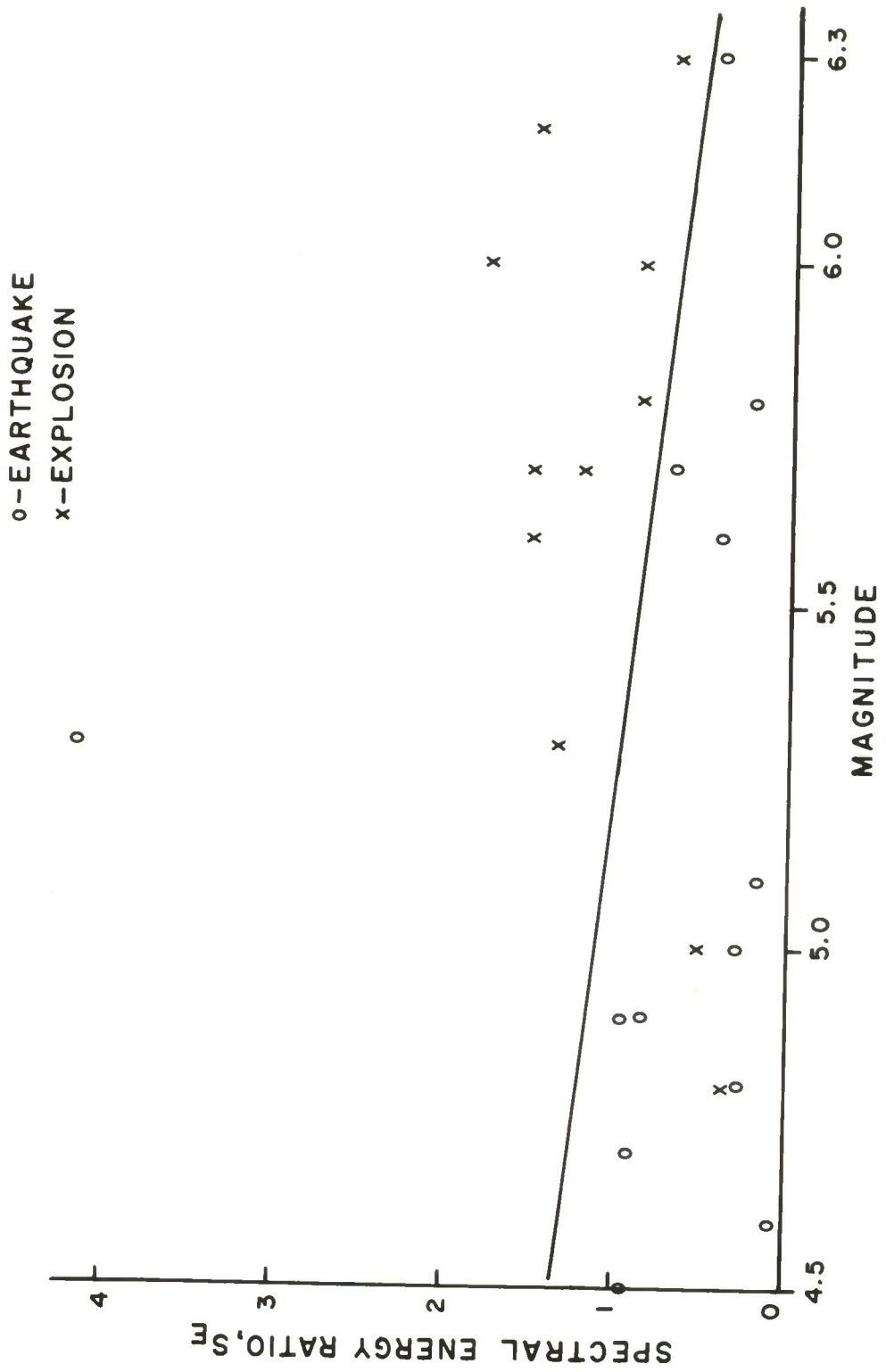ANALOG ARRAY (UNFILTERED)

o-EARTHQUAKE
x-EXPLOSION

FIGURE 4.17
SPECTRAL ENERGY RATIO TEST
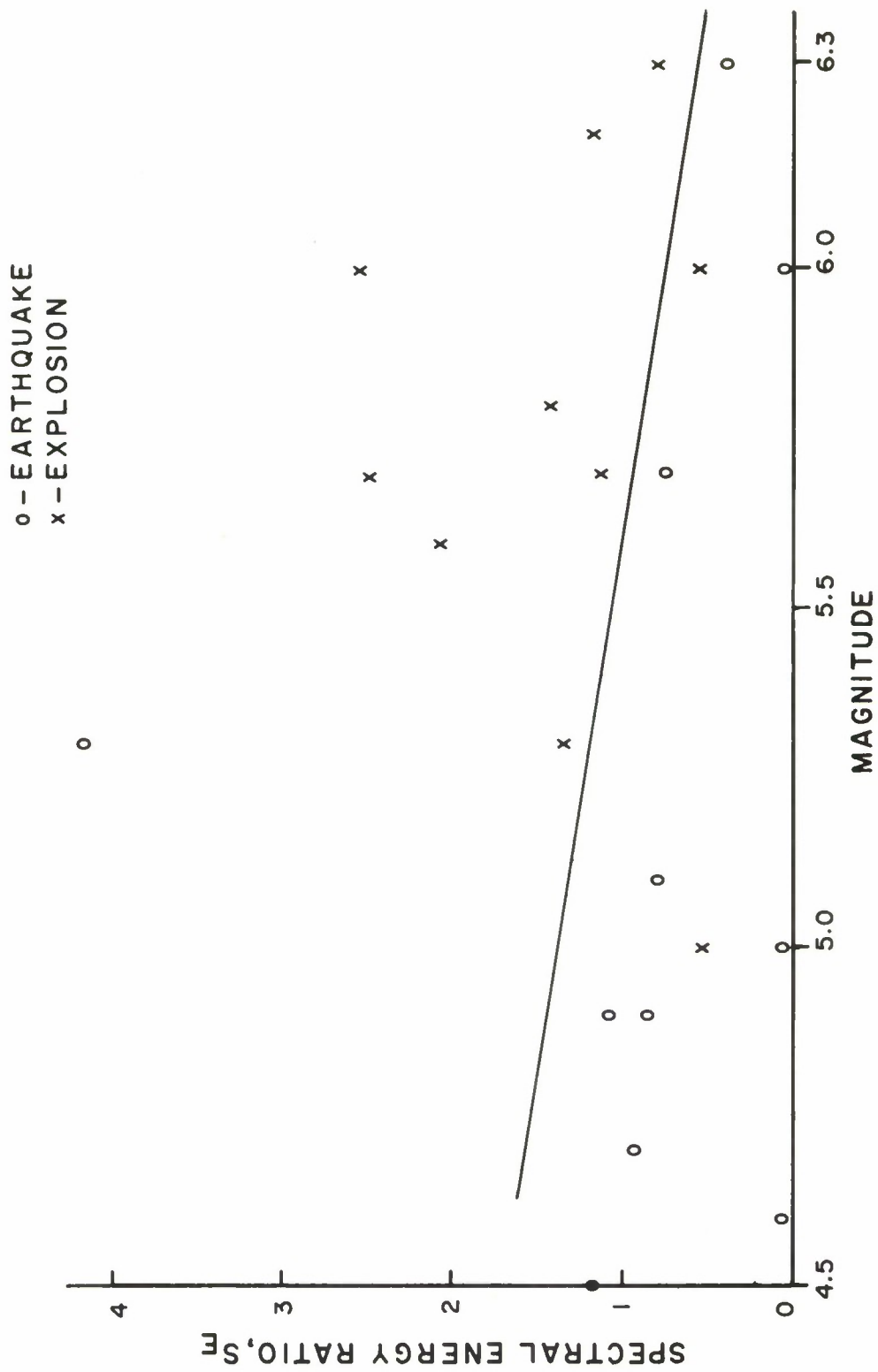DIMUS ARRAY (UNFILTERED)

MAGNITUDE

SPECTRAL ENERGY RATIO, S_E

FIGURE 4.18
SPECTRAL ENERGY RATIO TEST
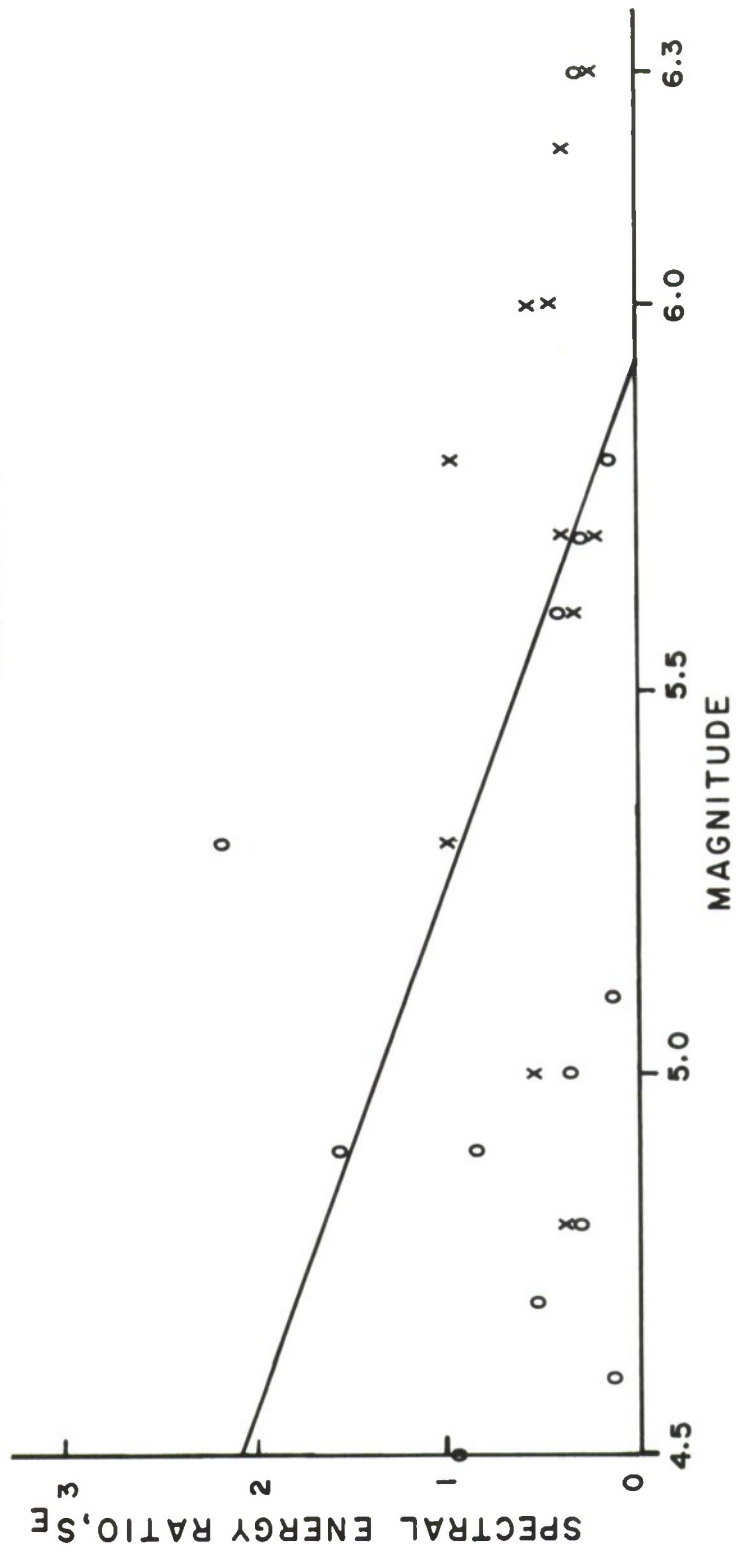MOD-DIMUS I ARRAY(UNFILTERED)

o-EARTHQUAKE
x-EXPLOSION

FIGURE 4.19
SPECTRAL ENERGY RATIO TEST
MOD-DIMUS 2 ARRAY(UNFILTERED)

of using the envelope of the single analog channel for scaling will be examined. Also, it may be possible to improve the results obtained for the spectral ratio test by varying the locations of the filters H_1 and H_2. This possibility will be examined. If possible, additional seismic events will be included in the study.

SECTION V

EXTENDED AUTOMATIC pP TEST

The previously reported work[13] on an automatic pP test for shallow earthquakes has recently been extended. In essence, this test consists of scanning an array of continental dimensions for events of known location, with depth as a parameter. A depth limitation of 40 km applied to the original test since a constant velocity of propagation above the focus of the event was assumed. Because depth determinations based only on arrival time information are often not of sufficient quality to allow reliable discrimination between surface-focus events and earthquakes shallower than 100 km, an extension of the pP test to depths below 40 km is clearly desirable. It should be noted that for discrimination purposes, fairly large errors in depth estimates may be tolerated for deep events. That is, the difference between 60 and 80 km is unimportant, but the difference between 0 and 20 km is quite important in deciding whether an event is an earthquake or an underground nuclear test.

To date the extended test has been applied to five events using only data from LASA-Montana. The results of these calculations are inconclusive, but it is anticipated that calculations based on continental-size arrays will lead to satisfactory results.

5.1 DESCRIPTION OF TEST AND DATA

Two changes were made to permit the test to function to depths of 150 km. When the test depth exceeded 33 km, the mean depth of the Moho, the constant velocity assumption was dropped, and average velocities above and below the Moho were assumed. Phasing times were then calculated using both these two assumed velocities and the J-B travel-time tables. For these depths the energy in the test-depth window was compared to the average energy in two five-second intervals (one preceding and one following the test depth) rather than in the fixed interval from three to thirteen seconds used for the shallower test depths.

It is expected that the pP test would function best with a continental-size array. The reasons for this are twofold, and both relate to the desired enhancement of pP compared to coda. With arrays of continental dimensions the coda waveforms at the various seismometers will be much less correlated than, for example, in the case of LASA-Montana. Secondly, the moveout of the P-phase increases with the aperture of the array. For a continental-size array it may be large enough to assist in the identification of this phase. With LASA, for example, at most 0.2 sec moveout is possible, and this is not sufficient to help in the identification of the pP phase.

Since relatively long records are required in order to include pP from deep earthquakes, the necessary data to apply this test with continental-size arrays have not been immediately available. For this reason, only data from LASA-Montana have been used to date. These data have been sufficient to suggest that the test will work properly when the signal-to-noise ratio is adequate. It is anticipated that the performance of the test will improve substantially when data from continental-size arrays are used.

Five medium depth earthquakes have been processed. Table I summarizes information concerning these events. In order to study the dependence of this test on the number of stations, two calculations were performed for each event. For one set of calculations the center elements of the AO and F-ring clusters were used. The other set included these five elements plus the four center elements of the C-ring cluster. The first set should involve the minimum coherence between coda signals since the seismometers are separated by approximately 100 km. The second set should allow better signal-to-noise enhancement, but will suffer from a higher value of coda correlation.

5.2   EXPERIMENTAL RESULTS

One measure of the effectiveness of the automatic depth test is a comparison with the C&GS reported depths. Where this reported depth was based on the differential arrival times of the P and pP phases of the earthquake, the two depth determinations should agree. Where the reported depth is the result of an unrestrained (in depth) epicenter calculation, however, the 30 to 40 km standard deviation in the reported depth will result in differences in the two measurements. Here, the difference need not be considered as an error in the automatic test results.

Figures 5.1 through 5.5 show the values of the test statistic as a function of depth for the five events studied. Also shown on the figures are the C&GS reported depths. The 23 November 1965 event (Figure 5.1) was quite small (magnitude 4.3). As a result, the signal-to-noise ratio was not sufficient to produce strong peaks. The improvement in signal-to-noise ratio in going from the five to the nine-station test, however, is apparent in the figures. The 17 June 1966 event (Figure 5.2) exhibits two marked peaks in the test statistic. The shallower of the two, 60 km, corresponds quite well with the reported depth. Here, the reported depth was restrained on the basis of two stations with emergent pP picks giving depths of 62.4 and 70.8 km, respectively. The second peak corresponds exactly to the differential time delay for the sP phase. The 7 January 1966 event (Figure 5.3) is similar to the 23 November event in that the low signal-to-noise ratio prevents the test statistic

TABLE I - EVENTS USED FOR AUTOMATIC pP TEST

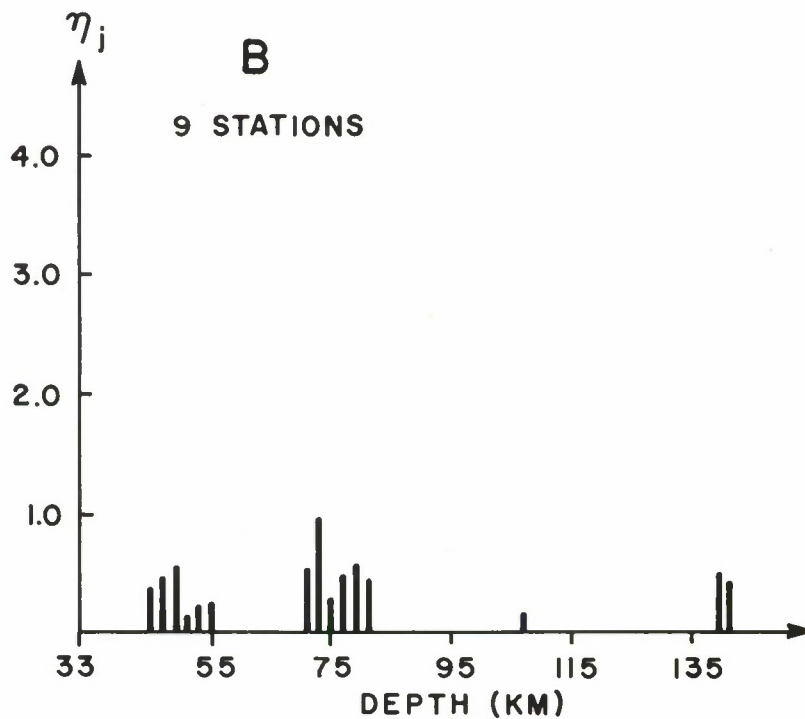| Date	Region	Lat	Lon	Origin Time	Depth	Mag
23 Nov 65	Andreanof Island	51.4N	179.9W	6/16/26.0	33	4.3
11 Dec 65	Kurile Islands	50.5N	155.3E	12/16/59.9	110	4.9
30 Dec 65	South Peru	16.8S	71.2W	6/16/3.9	118	5.7
7 Jan 66	E. Cst. Kamchatka	52.6N	160.0E	7/45/27.3	92	5.1
17 Jun 66	Hokkaido	42.4N	142.9E	8/48/33.2	67	4.8

A

23 NOV 65
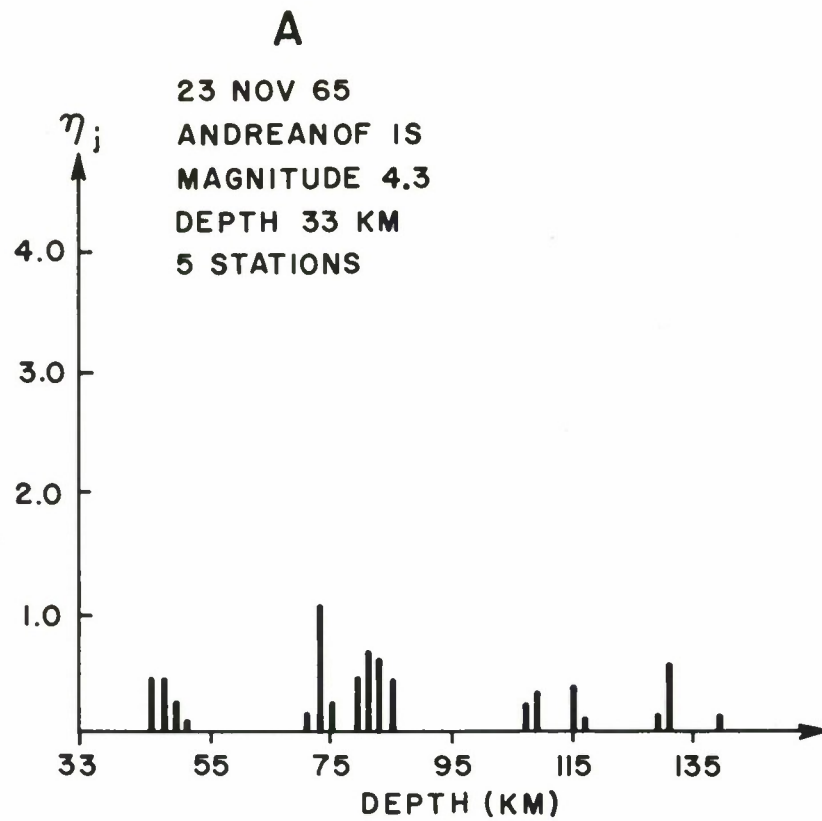ANDREANOF IS
MAGNITUDE 4.3
DEPTH 33 KM
5 STATIONS

B

9 STATIONS

FIGURE 5.1 (A-B)
EXTENDED AUTOMATIC pP TEST
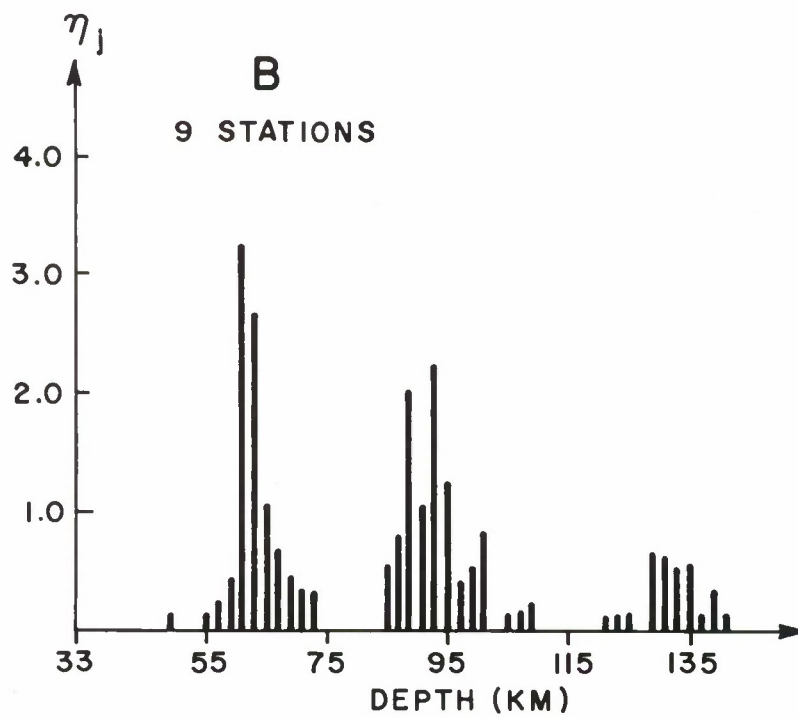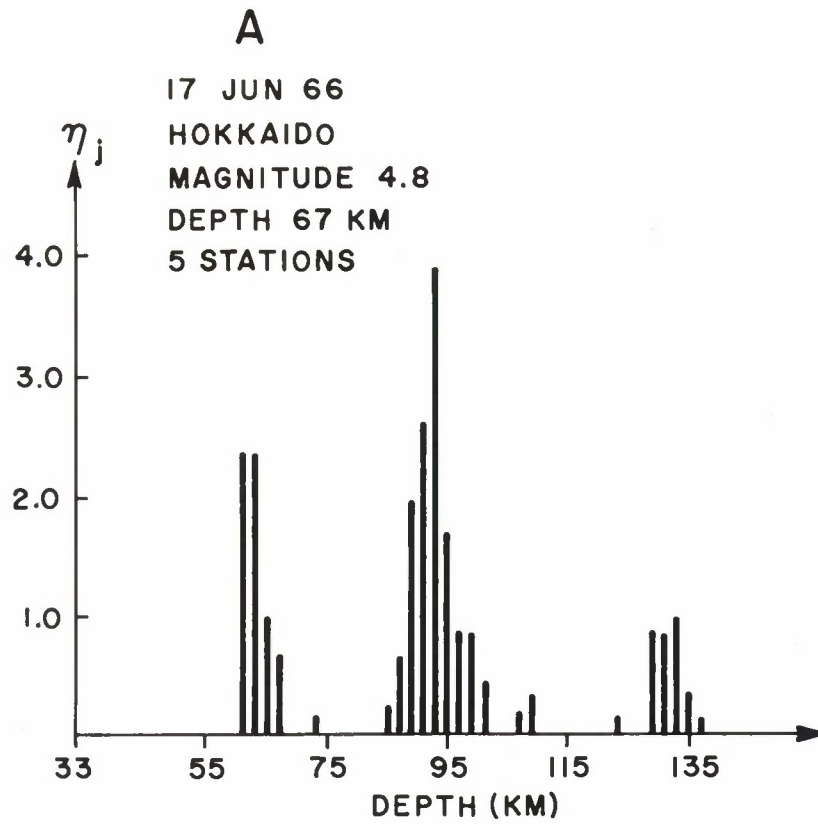
FIGURE 5.2 (A-B)
EXTENDED AUTOMATIC pP TEST
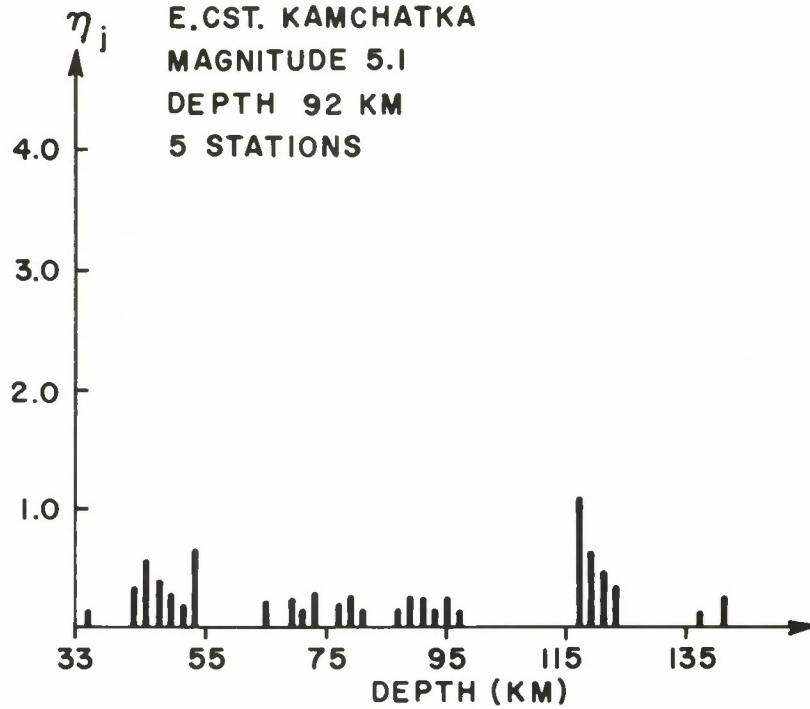
FIGURE 5.3 (A–B)
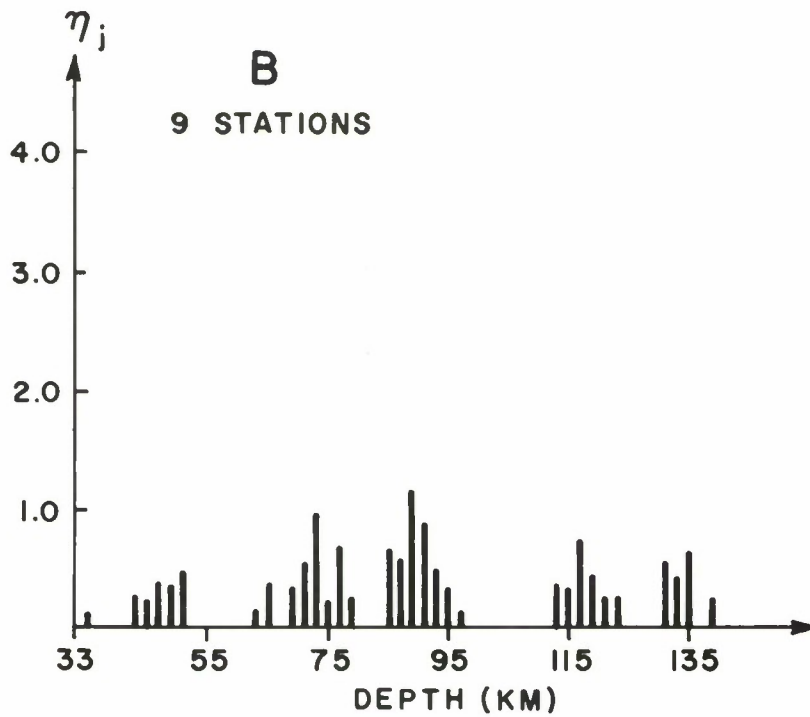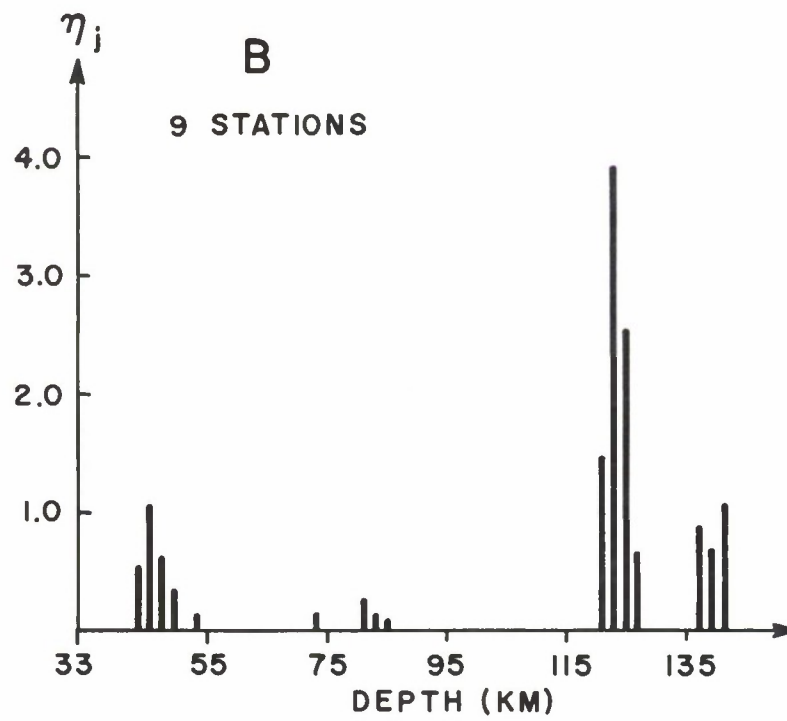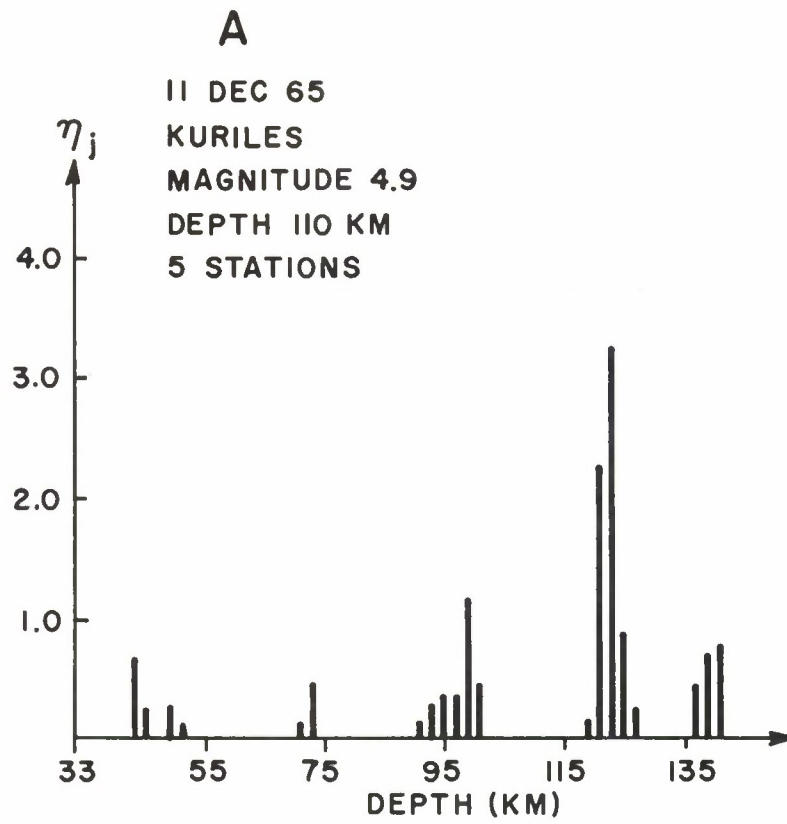EXTENDED AUTOMATIC pP TEST
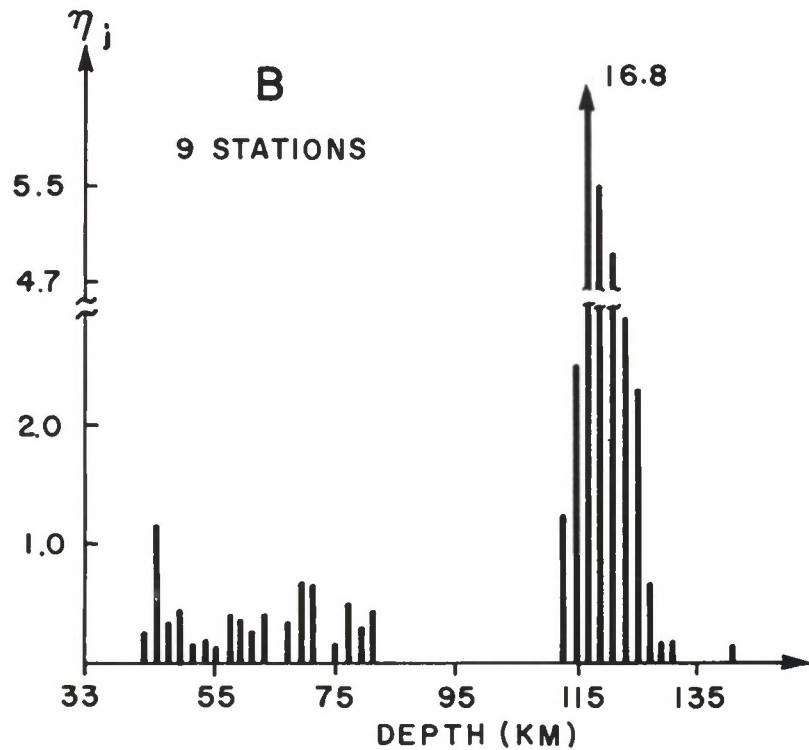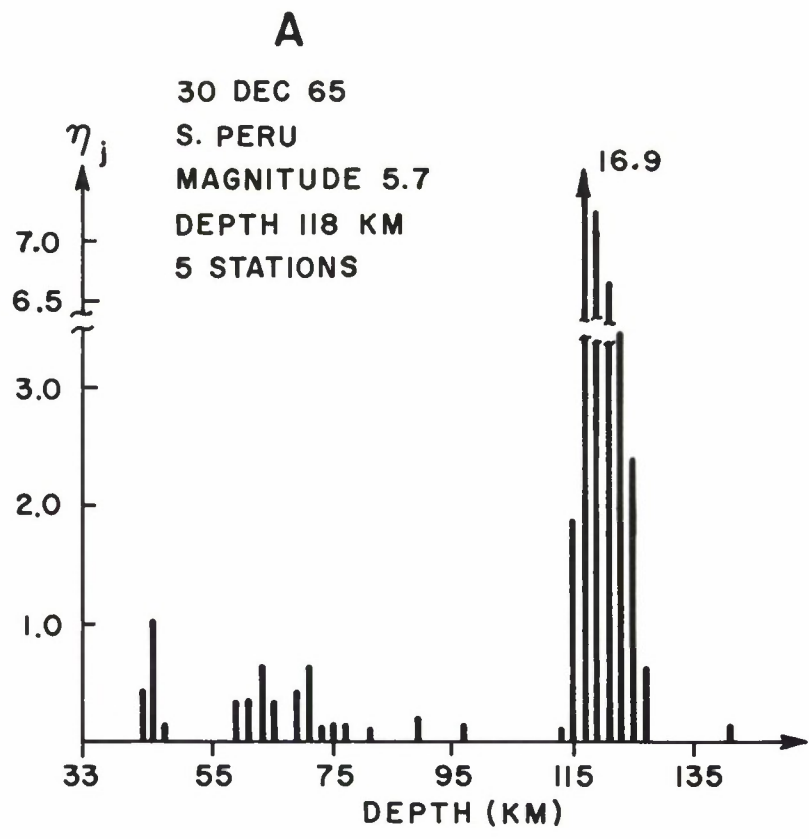
FIGURE 5.4 (A-B)
EXTENDED AUTOMATIC pP TEST

FIGURE 5.5 (A-B)
EXTENDED AUTOMATIC pP TEST

from peaking enough to make a depth pick. The 11 December 1965
event (Figure 5.4) shows only one strong peak in the test sta-
tistic at a depth of 123 km. This is in good agreement with
the 110 km reported depth which resulted from the identification
of the pP phase at one station by C&GS. Finally, the 30 December
1965 event (Figure 5.5) shows a single, exceedingly strong peak
in the test statistic for exactly the reported depth. This is to
be expected, since the reported depth was restrained on the basis
of five pP-phase identifications by C&GS, and the signal-to-noise
ratio for this event was large.

5.3   SUMMARY AND CONCLUSIONS

The pP test has been extended and applied to LASA data
from five earthquakes. For two of the events, poor signal-to-
noise ratio appears to have prevented any clear peaks in the
test statistic. While it is likely that the correct depth cor-
responds to one of the observed maxima in the test statistics,
no reliable depth pick is possible. It may be that these results
would improve significantly if filtering were used to improve the
signal-to-noise ratio of the original seismograms. For the
three events with adequate signal-to-noise ratios, correct depth
picks were easy to obtain using this test.

It is anticipated that the use of larger arrays will
result in substantial improvement in the performance of this
test, provided that the pP alignment procedure is sufficiently
accurate to handle the deeper earthquakes. In particular, the
increased moveout of pP across the larger array should alleviate
the problems of multiple peaks, except in the case where sP
appears, and this case can be recognized and treated separately.

REFERENCES

[1] "Large Aperture Seismic Arrays," General Atronics Corporation, June 1967, pp. 139-158.

[2] *Ibid.*

[3] *Ibid.*, pp. 158-166.

[4] *Ibid.*, pp. 78-82.

[5] J. Capon, R.J. Greenfield, R.T. Lacoss, "Design of Seismic Arrays for Efficient On-Line Beamforming," Lincoln Laboratory Technical Note 1967-26, 27 June 1967, pp. 2-5.

[6] C.B. Forbes, R. Obenchain, R.J. Swain, "The LASA Sensing System Design, Installation, and Operation," *Proc* IEEE, *53* December 1965, p. 1839.

[7] General Atronics, *op. cit.*, pp. 45-49.

[8] *Ibid.*

[9] *Ibid.*, pp. 78-94.

[10] *Ibid.*, pp. 124-138.

[11] *Ibid.*

[12] P.E. Green, "Semiannual Technical Summary Report to the Advanced Research Projects Agency on Seismic Discrimination," Lincoln Laboratory, M.I.T., 31 December 1966, p. 7.

[13] General Atronics, *op. cit.*, pp. 95-123.

DOCUMENT CONTROL DATA - R & D

(Security classification of title, body of abstract and indexing annotation must be entered when the overall report is classified)

1. ORIGINATING ACTIVITY (Corporate author)	2a. REPORT SECURITY CLASSIFICATION
General Atronics Corporation 1200 East Mermaid Lane Philadelphia, Pennsylvania 19118	Unclassified
	2b. GROUP N/A

3. REPORT TITLE

FIRST QUARTERLY TECHNICAL REPORT -
LARGE APERTURE SEISMIC ARRAYS (LASA)

4. DESCRIPTIVE NOTES (Type of report and inclusive dates)

Quarterly Report

5. AUTHOR(S) (First name, middle initial, last name)

None

6. REPORT DATE	7a. TOTAL NO. OF PAGES	7b. NO. OF REFS
September 1967	73	4

6a. CONTRACT OR GRANT NO.	9a. ORIGINATOR'S REPORT NUMBER(S)
F19628-67-C-0370	ESD-TR-67-615
b. PROJECT NO.	
c.	9b. OTHER REPORT NO(S) (Any other numbers that may be assigned this report)
d.	

10. DISTRIBUTION STATEMENT

This document has been approved for public release and sale; its distribution is unlimited.

11. SUPPLEMENTARY NOTES	12. SPONSORING MILITARY ACTIVITY
	Directorate of Planning and Technology, Electronic Systems Division, AFSC, USAF, L G Hanscam Fld, Bedford, Mass. 01730

13. ABSTRACT

Four topics are discussed in this Quarterly Progress Report. The first topic related to the "high-frequency" (4-5 Hz) portion of LASA seismograms. Data are cited which indicate a statistically significant amount of signal energy in this region, and preliminary unsuccessful efforts at combining high-pass filtered records from nearby seismometers are described. The second topic is the problem of detecting underground nuclear tests in the presence of large natural events. A hypothetical detection system consisting of a number of single seismometers at close range and a continental-size array at teleseismic range is analyzed and discussed. The third topic is DIMUS processing of seismic array outputs. The conventional DIMUS processing consists of hardlimiting each seismogram (thereby yielding a one bit per sample representation) and then proceeding as with the unaltered seismograms. Two modified DIMUS schemes, which require a single analog channel, are considered. The performance of these schemes, conventional DIMUS, and conventional analog arrays is evaluated for the spectral-ratio and complexity diagnostics. Finally, an extended version of an automatic pP test is discussed. Initial calculations are presented that suggest that this test will yield satisfactory depth picks for earthquakes as deep as 150 km.

DD FORM 1473
1 NOV 66

14. KEY WORDS	LINK A		LINK B		LINK C	
	ROLE	WT	ROLE	WT	ROLE	WT
Seismology Arrays Signal Processing Spectral Analysis Seismic Wave Propagation Seismic Discrimination						